

ASSESSING VISCOELASTIC PROPERTIES OF
CHITOSAN SCAFFOLDS AND VALIDATING
SEQUENTIAL AND CYCLICAL TESTS

By

SWAPNIKA RATAKONDA

Bachelor of Technology in Chemical Engineering

Dr. B. V. Raju Institute of Technology

(Affiliated to Jawaharlal Nehru Technological University)

Andhra Pradesh, India

2009

Submitted to the Faculty of the
Graduate College of the
Oklahoma State University
in partial fulfillment of
the requirements for
the Degree of
MASTER OF SCIENCE
December, 2011

ASSESSING VISCOELASTIC PROPERTIES OF
CHITOSAN SCAFFOLDS AND VALIDATING
SEQUENTIAL AND CYCLICAL TESTS

Thesis Approved:

Dr. Sundar V. Madihally

Thesis Adviser

Dr. R. Russell Rhinehart

Dr. Joshua D. Ramsey

Dr. Sheryl A. Tucker

Dean of the Graduate College

TABLE OF CONTENTS

| Chapter | Page |
|---|------|
| I. INTRODUCTION..... | 1 |
| II. BACKGROUND..... | 8 |
| Tissue Engineering..... | 8 |
| Scaffolds | 10 |
| Natural Polymers | 12 |
| Chitosan..... | 13 |
| Gelatin | 13 |
| Collagen..... | 14 |
| Synthetic Polymers | 14 |
| Composite Polymers | 15 |
| Generating Scaffolds..... | 15 |
| Electrospinning | 15 |
| Solvent Casting and Particulate leaching..... | 16 |
| Phase Separation | 16 |
| Lyophilization | 17 |
| Mechanical Properties of Scaffolds | 17 |
| Viscoelasticity..... | 18 |
| Tensile Strength | 21 |
| Stress-Relaxation Behavior..... | 22 |
| Cyclic Behavior | 23 |
| Viscoelastic Models | 23 |
| III. METHODOLOGY | 26 |
| Materials and Methods..... | 26 |
| Materials | 26 |
| Formation of Scaffolds..... | 26 |
| Mechanical Testing | 27 |
| Microstructure Characterization..... | 28 |
| Modeling..... | 30 |
| Pseudo-component Models | 30 |
| Mathematical Statement | 32 |

| Chapter | Page |
|--------------------------------------|------|
| IV. RESULTS | 38 |
| Tensile Testing..... | 38 |
| Stress-Relaxation Behavior..... | 39 |
| Model Parameter Values..... | 43 |
| Cyclic Behavior | 45 |
| V. DISCUSSION | 49 |
| VI. CONCLUSION AND FUTURE SCOPE..... | 54 |
| Conclusions..... | 54 |
| Future Scope | 55 |
| REFERENCES | 56 |
| APPENDICES | 61 |

LIST OF TABLES

| Table | Page |
|---|------|
| 1. Parameter and SSD values of 5-parameter Model..... | 43 |
| 2. Parameter and SSD values of 8-parameter Model..... | 44 |

LIST OF FIGURES

| Figure | Page |
|--|------|
| 1. Summary of the current study..... | 7 |
| 2. Basic Principle of Tissue Regeneration..... | 10 |
| 3. (a) 3-D scaffold (b) porous structure of scaffold..... | 11 |
| 4. (a) Sources of Chitosan (b)porous structure of chitosan..... | 13 |
| 5. (a) PCL (b) microstructure of PCL..... | 14 |
| 6. Stress-strain behaviors of (a) elastic and (b) viscoelastic materials during loading and unloading..... | 19 |
| 7. General stress-strain or tensile behavior of a material showing (a) elastic region, (b) plastic region and (c) failure..... | 22 |
| 8. Solvent Casting of chitosan scaffolds using hydrochloric acid and freezing..... | 27 |
| 9. Micrographs of scaffolds showing porous structure before and after ramp and hold experiment..... | 29 |
| 10. Schematic interpretation of Non-linear response of stress with increase in strain..... | 31 |
| 11. Model with (a) one hyper elastic spring and a retain pseudo-components (b) one hyper elastic spring and two retain pseudo-components in parallel..... | 32 |
| 12. Stress-strain behavior of scaffolds in hydrated conditions..... | 39 |
| 13. Dynamic behavior of different scaffolds and comparison of model predictions to the experimental representative (n=4)..... | 40 |
| 14. Stress relaxation function, $G(t)$, plot from the characteristic trend of the first cycle of each strain rate..... | 41 |
| 15. Relaxation behavior of scaffolds in different stages of ramp and hold tests..... | 42 |
| 16. Cyclic behavior of different scaffolds and comparison of model predictions..... | 46 |

CHAPTER I

INTRODUCTION

On a daily basis we see people getting injured in road accidents or fire accidents and having organ failures due to poor health. Whatever the reason may be, millions of people need some kind of tissue or organ repair due to these damages. The general treatments for these failures are i) surgery, ii) replacing the failed organ by a mechanical device, or iii) organ transplantation.

However common these treatments are they have many associated limitations. For example surgical reconstruction may accompany with lot of pain, discomfort and time to heal. Also the visible scars of the surgery will remain forever causing mental disturbance to the patients. Replacing failed organs like heart, lungs or kidneys by mechanical devices that function like them has also been implemented, but a mechanical device can never be able to replace the biological activities of the organs and body. And, having a machine connected to you all the time is very discomfoting and will not last long. In case of organ transplant, there is a shortage of organ donors.

In the US alone there are still 104,748 people waiting for an organ transplant and 18 people die each day waiting for an organ transplant [1]. Considering all these problems, research has been developed in the area of tissue engineering as an alternative to tissue or organ repair. Tissue engineering is a fast growing area in which the combinations of materials, cells and engineering are used to improve or replace biological activity [2]. Tissue engineering can be applied to repair bones, nerves, skin, cartilage, etc [3]. This involves developing a cellular matrix outside the body first and then introducing it to the body. The cells are cultured on three-dimensional biodegradable scaffolds. With the availability of different natural and synthetic materials that can be introduced to human body, regenerating defective tissues outside the body has attracted significant interest.

Three dimensional scaffolds can be prepared from both synthetic and natural materials that are i) compatible with the human body, ii) bio-degradable and iii) supportive of reparative cell colonization [4-5]. Apart from being bio-compatible, tissue engineering scaffolds should have high porosity in order to aid biological activities and be mechanically strong to withstand the stresses and strains in the body [4]. Though synthetic materials can be formed into mechanically strong porous scaffolds, they are not as supportive to biological activities as their natural counterparts [6-9]. Naturally available chitosan-based scaffolds have acquired significant consideration due to various advantages including cost, availability and biocompatibility [10]. Chitosan is derived from naturally occurring chitin present in crabs, shrimp, lobsters, etc. Chitosan is a bioactive, biocompatible, and biodegradable polysaccharide [11]. Chitosan mimics the extracellular matrix (ECM) and is readily available [5, 12]. Chitosan can be processed

into beads, gels, fibers or films [13-15], and the required porous microstructure, biological activity and mechanical strength of chitosan can be achieved by varying the concentration of chitosan, degree of deacetylation, and blending with other materials [5]. Gelatin is derived by irreversibly hydrolyzing collagen present inside an animal's skin, intestines, connective tissue and bones; and hence, gelatin derived from collagen will enhance cellular activity. Gelatin contains Arg-Gly-Asp (RGD) like sequence that promotes cell adhesion and migration which makes it an ideal candidate for tissue engineering [9]. Gelatin based grafts have been used in tissue engineering. It has, however, lower mechanical strength and is soluble in aqueous media. It is therefore usually cross-linked with other scaffold substances to apply in tissue-engineering [7-8, 10].

For example, chitosan-gelatin scaffolds have also been used [12, 16] to incorporate cell adhesion and migration properties of gelatin [17-19]. Some chitosan-gelatin scaffold preparations use cross-linkers to strengthen the bonding between the two components [16] but the cross-linkers such as glutaraldehyde increase the stiffness of 3D structures and also promote calcification. It has been shown in the previous studies that gelatin-chitosan complexes can be formed without cross-linkers and extensive analyses show stability and functionality [20]. Cellular activities of human fibroblasts and endothelial cells have shown the possibility of using chitosan and chitosan-gelatin scaffolds [20-23].

Hence chitosan and gelatin have the ability to increase cellular activity and are a good choice for tissue engineering applications [24]. In this study, gelatin has been mixed together with chitosan to form a chitosan-gelatin scaffold to see if addition of

gelatin alters the mechanical properties of chitosan. The scaffolds have been prepared using a lyophilization (Freeze Drying) technique. This is a very easy and cost-effective method. Chitosan and gelatin scaffolds have been attained in the past with this method and this method gives a good 3D porous structure [5]. Pore sizes attained by freeze drying scaffolds in the concentration range of 0.5 wt% and 2 wt% are apt for the cellular activity. Hence, these concentrations were used in the study.

Biological tissues display a complex mechanical behavior in that they exhibit both viscous (like fluids) and elastic (like solids) behavior, a property termed as viscoelastic behavior. Viscoelastic behavior is time-dependent and load-history-dependent, a well-studied characteristic of human tissues [25-28]. The viscoelastic properties of tissues create an environment for cells which is critical for their viability and function. Knowing how tissues in the body function is crucial to develop models which make estimation of performance of the tissue during stress and strain easier and can be used in many applications like injury prevention in automobiles, earplugs, sports, etc. When a tissue is being replaced by an external scaffold for tissue regeneration, then understanding the viscoelastic behavior of the scaffold material is necessary to know how it performs during various applications. Significant research has also been done in developing the mathematical models to understand the complex mechanical behavior [28-31], and modeling the experimental viscoelastic behavior of the material can help in monitoring the changes in the stress-strain behavior of the scaffold that is placed in the body. To account for the *i*) stress-relaxation with time under a constant strain rate, *ii*) the deformation of the material shape under constant load, *iii*) the gradual return of the material to its original form once the load is released, *iv*) effect of cells, matrix, etc. on

tissues and v) their inconsistent tissue properties; time-dependent, non-linear, multi-component viscoelastic models are essential. Many studies assessed the linear viscoelasticity of chitosan solutions [32], films [33-34], hydrogels [35-37], or scaffolds [38] with and without blending other biomaterials, by performing experiments at various frequencies but their non-linear viscoelastic behavior has not been completely addressed. So in this study, the chitosan scaffolds have been tested for their mechanical strength. In the mechanical testing the scaffolds were analyzed by tensile, stress-relaxation and cyclical testing. These properties were modeled using the two developed models (8-parameter Model and 5-parameter Model). These models were developed to be compatible with observations of the micro-structure deformation of the scaffolds during the mechanical testing. The same models were also used to predict cyclical properties of the scaffolds.

The objective of this study was to evaluate and model the viscoelastic characteristics of chitosan and chitosan-gelatin scaffolds prepared using freeze-drying. Based on the pore characteristics required for tissue regeneration, scaffolds made of 0.5 wt% and 2 wt% were evaluated to assess the effect of polymer concentration may affect the material. The study can be divided into three aspects.

1. The stress relaxation properties of both chitosan and chitosan gelatin were evaluated and compared to see if addition of gelatin alters the mechanical properties of chitosan.
2. The 8-parameter and 5-parameter models were made to fit the stress-relaxation properties of chitosan and chitosan-gelatin scaffolds and were compared to see which gave a better fit.

3. Both the models were used to predict the cyclical properties of the scaffolds and compared to see which gave a better prediction for each concentration.

In summary, chitosan and chitosan-gelatin scaffolds were tested for their viscoelastic properties using tensile, stress-relaxation and cyclical testing. The developed models were used to fit stress-relaxation behavior of the scaffolds and were used to predict the cyclical properties. These predicted properties were compared with the experimental cyclical properties. The schematic of the above summary is shown in **Figure 1**. The figure shows examples of stress-relaxation and cyclic behavior of the scaffolds. In all, the 8-parameter model gave a better fit to the stress-relaxation data and gave better cyclical prediction than the 5-parameter model. But the cyclical prediction was accurate only for the 2 wt% scaffolds and not the 0.5 wt% scaffolds.

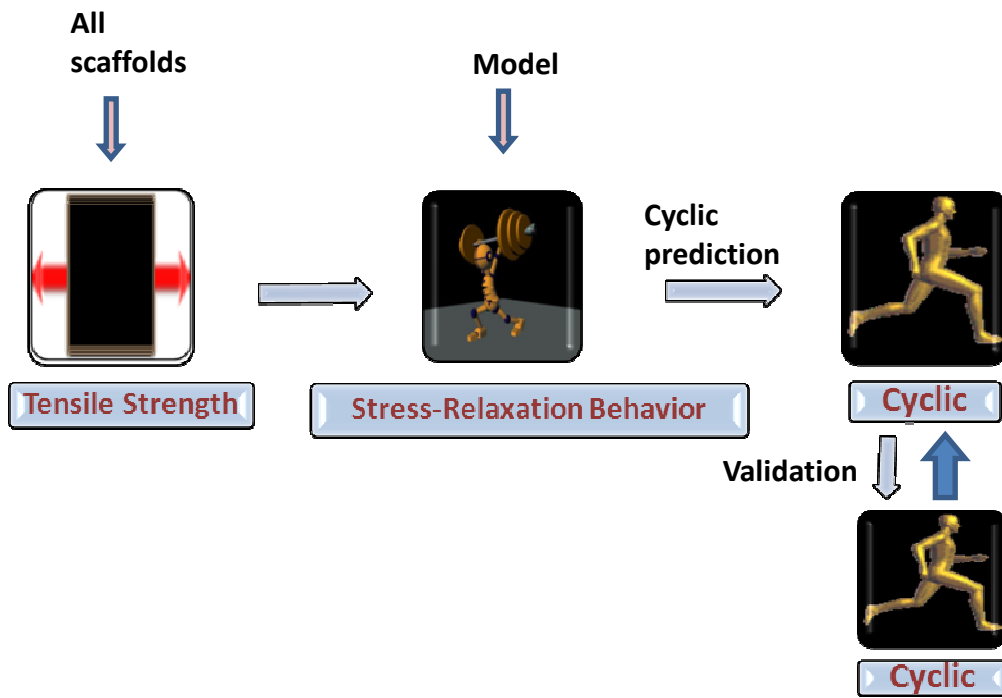


Figure 1: Summary of the current study

CHAPTER II

BACKGROUND

Tissue Engineering

Many suffer with tissue or organ failures due to ill-health or various accidents. To treat these, most common treatment methods are surgical reconstruction, replacing the organs with mechanical devices and organ transplantation. But certain limitations of these methods have created interest in the area of tissue engineering. Learning more about tissue engineering and developing the research in this field will help in introducing an efficient method to treat tissue or organ failures.

Tissue regeneration is a part of tissue engineering in which we develop different methods to aid regeneration of damaged tissues in the human body. Every species is capable of regeneration, from bacteria to humans [39-40]. This can be used as an advantage to repair defective or damaged tissues in a human body with help of different procedures. With a source that can aid regeneration of tissues, humans can regenerate lost finger tips, livers, ribs, cartilages, skin and bones [41-48]. Further in this section the methodology and principles, that can aid tissue regenerations, have been explained.

Tissue engineering is defined as “an interdisciplinary field that applies the principles of engineering and life sciences toward the development of biological substitutes that restore, maintain, or improve tissue function or a whole organ”[2]. This discipline also needs a proper understanding of tissue growth and its regeneration to apply it for clinical use. With this understanding tissue engineering can be applied to tissue repair, replacement, maintenance and enhancement of tissue functions [49]. In summary, tissue engineering is the right combination of cells, materials and engineering that are used to improve or replace biological activity.

The basic principle of any tissue regeneration is shown in **Figure 2**. In a tissue regeneration process, stem cells are harvested from the body of a patient. These cells are cultured and differentiated using growth factors. The expanded cells are cultured on a 3D polymeric scaffold on which all the biological functions take place. Once the cells bind themselves and generate a graft, the whole item is placed at the injury site. In a successful process these cells grow and regenerate the tissue in the body. The figure shows the general procedure applied to regenerate a tissue at the defective site using a three-dimensional (3D) scaffold which acts as a support and matrix for all the cellular activity. One of the main challenges in tissue regeneration is to find the right scaffold that will carry out the required functions in the body, which is the basis of this study.

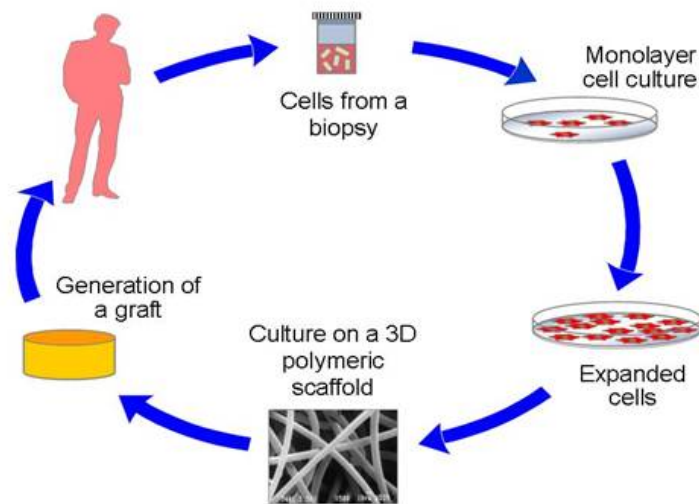


Figure 2: Basic Principle of Tissue Regeneration.

(Picture from: <http://webold.iitd.ac.in/~textile/highlights/fo18/01.htm>)

Scaffolds

As shown in **Figure 2** we need a medium or a support structure for the cellular activity to carry out tissue regeneration. This medium should be similar to the tissue matrix in our bodies. This support structure, termed as scaffold, provides a framework and initial support for the cells to attach, proliferate, differentiate and form an extracellular matrix (ECM)[50].

Scaffold is a structure that is capable of supporting three dimensional tissue formations when cells are seeded on it. Scaffold should have the appropriate physical, chemical and mechanical properties to enable cellular activity for tissue regeneration[3]. Also, scaffold matrices should exhibit similar morphology as that of a natural ECM (Extracellular matrix), which is responsible for the cellular function in the body and hence can be used for nerve, skin, blood vessel and tendon grafts [51].

Preparing a three dimensional scaffold that can restrain an assembly of reparative cells, is one of the major concerns. Scaffolds support biological processes like adhering, migrating, growing and differentiating of cells on the matrix which is responsible for attaining a proper binding between cells and scaffolds in order to generate a new tissue [52]. It also should be capable of delivering, retaining cells and biochemical factors and enabling diffusion of necessary cell nutrients[53].

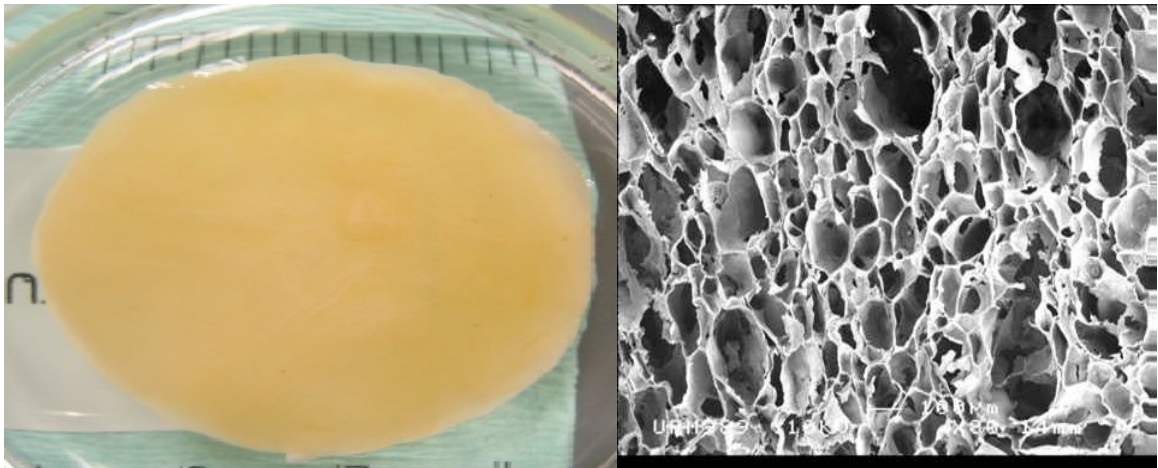


Figure 3: (a) 3-D scaffold (b) porous structure of scaffold.

To achieve the required cellular activity scaffolds should have the following characteristics:

- (1) Highly porous; so that cells can migrate, multiply and attach deep within the scaffolds.
- (2) Biodegradable; so that once the tissue is formed it should get out of the system without becoming toxic.
- (3) Biocompatibility; so that it does not affect the other parts of the body and has a high affinity for cells to attach and proliferate.
- (4) Right shape; so that it has the shape of the injury site in the body.

(5) Appropriate mechanical strength; so that it can withstand different strains and stresses in the body [53].

A variety of polymers synthesized from biomaterials are used to build biodegradable scaffolds. These can be categorized as naturally derived and synthetic polymers. The majority of materials usually used in tissue engineering are adapted from other surgical uses, such as sutures, haemostatic agents and wound dressings[54]. These include synthetic biodegradable materials, such as aliphatic polyesters (polyglycolic acid, polylactic acid and their co-polymers) and naturally derived materials such as collagen and chitin[55-56].

Natural Polymers

Natural polymers are mostly considered due to their biocompatibility, biodegradability, resemblances to the biological structures of ECM in the body and ability to aid in effective cellular activity [8]. These polymers are treated chemically to achieve the form of the substance we want that can be used to prepare a scaffold.

Natural Polymers are originated and derived from substances found in humans, plants or animals. Naturally derived polymers exhibit lower mechanical strength and most of them are hydrophilic and hence do not make great 3-D structures. By chemical treatment these polymers have to be converted to hydrophobic substances. Most common natural polymers used in tissue engineering are chitosan, gelatin and collagen.

Chitosan is bio active, biocompatible, biodegradable, antiseptic, mimics the ECM closely and readily available. It is produced commercially by deacetylation of chitin, which is found in abundance in most crustaceans. It is also available at a low cost.

Chitosan is a linear polysaccharide composed of randomly distributed β -(1-4)-linked D-glucosamine and N-acetyl-D-glucosamine. Most natural polymers become mechanically weak when hydrated, but chitosan and chitin are the exceptions. A highly porous structure of chitosan can be prepared easily by freezing and lyophilizing. However, the mechanical strength of chitosan is low when compared to synthetic polymers. But the required porous microstructure, crystallinity and mechanical strength of chitosan can be achieved by varying the concentration of chitosan, degree of deacetylation and freezing temperature [5]. Hence, it is being widely considered as a capable material for tissue engineering.



Figure 4: (a) Sources of Chitosan (b) porous structure of chitosan

Gelatin is also an active bio-component with biodegradability, biocompatibility and the ability to combine with other polymers without aid of an external solvent aid. It has lower mechanical strength and is soluble in aqueous media and hence is usually combined with other scaffold substances like chitosan to apply in tissue engineering [57]. Gelatin is derived from collagen by irreversibly hydrolyzing the latter and is available at low cost. Collagen is available inside an animal's skin, intestines, connective tissues and bones. Gelatin based grafts have been used recently in tissue engineering [58-60].

Collagen having high biocompatibility, biodegradability and that it makes up for the major component in a ECM [61] is considered one of the most capable materials and has been used for different applications. But, its low mechanical strength and fast rate of biodegradability have limited it from further use[62].

Synthetic Polymers

The main advantages of synthetic polymers are that they have high mechanical strength and a controllable degradation. They can also be formed into the required shapes and porous structure to create morphology that is close to an ECM [9]. These advantages have made them capable for research in tissue engineering recently [6-7, 9].

Polymers manufactured from various monomers by manufacturing are called synthetic polymers. However, synthetic polymers have a poor bio-regulating activity. One of the most common synthetic polymers that are used in tissue engineering are poly(glycolic acid) (PGA), poly(lactic acid) (PLA) and their copolymers and poly(caprolactone) (PCL). These mentioned polymers are biodegradable and approved by Food and Drug Administration for clinical use. Example of how PCL looks like is shown in **Figure 5**.

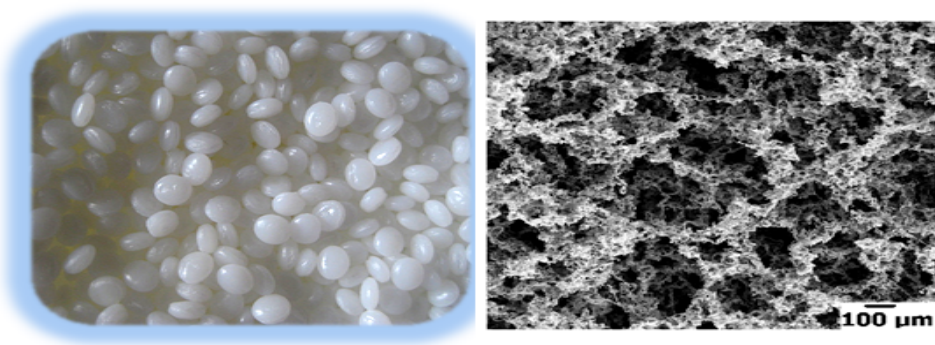


Figure 5: (a) PCL (b) microstructure of PCL

Composite Polymers

Synthetic polymers have high mechanical strength, bio-degradability and are easy to process but are poor in regulating cellular activity and on the other hand natural polymers have excellent at regulating biological activity but have poor mechanical strengths. Both synthetic and natural polymers have their own disadvantages. To cover up for these advantages, studies have been developed to combine both natural and synthetic polymers in order to have the bio-regulating activity of the natural polymers and give the mechanical strength of synthetic polymers [63-64]. Also studies were performed by combining two different natural polymers [7, 65] together to prepare scaffolds.

Generating Scaffolds

There are many methods that are used to fabricate scaffolds. The technique should be considered in such a way that it produces the scaffold with all the properties necessary for tissue regeneration. Scaffold characteristics such as porosity, interconnectivity, pore size, and surface roughness influence cellular responses should be met once the scaffolds are fabricated. There are many traditional techniques that have been use to synthesize scaffolds and some of them are listed below.

Electrospinning

Electrospinning has evolved into a very effective technique for producing well-controlled and organized nanofiber matrix depending on the application with the help of an appropriate set-up [66-67]. This cost-effective technique has the ability to vary the architecture of the matrix my varying simple properties of the whole set-up depending on

the type of application we are looking at. Due to its simplicity and versatility electrospinning is being considered as a potential method to produce 3D scaffolds in tissue engineering. Electrospinning produces more than 90% porosity and which allows efficient delivery of a loaded drug. Also, nanofiber scaffold matrices exhibit similar morphology as that of a natural ECM (Extracellular matrix), which is responsible for the cellular function in the body and hence can be used for nerve, skin, blood vessel and tendon grafts [51]. Nanofibers have various applications like filtration, protective materials, textiles, drug delivery, scaffolds for tissue regeneration and wound dressing material [51, 68]. Therefore, this is an efficient method to construct such nano scale scaffolds for biomedical applications. However, it has disadvantages like jet instability and packaging, shipping, handling and

Solvent Casting and Particulate Leaching

It is a process in which salt crystals are dissolved into a polymer matrix using a solvent. The solvent is allowed to evaporate leaving behind a polymer matrix with salt particles embedded throughout. The composite is then immersed in water where the salt leaches out to produce an interconnecting porous structure. Highly porous structures and large range of pore sizes can be attained from this method but has a poor control over internal architecture [69].

Phase separation

A biodegradable polymer is dissolved in molten phenol or naphthalene and biologically active molecules can be added to the solution. The temperature is then

lowered to produce a liquid-liquid phase separation and quenched to form a two-phase solid. The solvent is removed by sublimation to give a porous scaffold with bioactive molecules incorporated in the structure. This method also has limited control over internal architecture [69].

Lyophilization

It is one of the traditional methods which is cost-effective and easy. In this process the solution is allowed to freeze in the required shaped container or made in the form of a mould. During freezing ice crystals grow within the solution. The frozen or crystallized solution is put in a vacuum drier. Under high vacuum the water particles (ice phase) are removed from the solution which leaves behind the interconnected pores. This leaves a porous 3D structure of the scaffold. This method also known as freeze drying prevents reabsorption of moisture and action of micro-organisms. So the scaffold can be stored without any damage for a long time. With this method we can alter the porous structure with the change in concentration of the solution. In this study freeze drying has been used to prepare the scaffolds [5, 69].

There are many other methods like melt molding, gas foaming, template synthesis but the above are few of the mostly used methods.

Mechanical Properties of Scaffolds

The mechanical properties of tissues are different and are function specific in the body. Soft organic tissues have complex mechanical behavior. The elastic properties of tissues and the organs depend on the type of tissue and the function it performs and hence

properties of each tissue are varied. Also soft tissues have water in different percentages, and so the mechanical properties are affected by it. Hence, all mechanical testing of scaffolds should be done in hydrated conditions [70]. They often have a layered or an even more intricate makeup. They show nonlinear, viscoelastic behavior. So understanding the mechanical properties of scaffolds is important, to know its application [71-73].

Viscoelasticity

All mammalian tissues behave differently than other materials when they undergo deformation. For example, when a purely elastic material is stretched for some time and is relieved of stress it goes back to its original shape “instantaneously”. This gives a linear stress-strain behavior. But, when a tissue is stretched its stress-strain behavior is nonlinear and doesn’t go back to its original shape immediately. That means its behavior is time dependent. This behavior of tissues is due to their viscoelasticity. If scaffolds are being used in place of tissues for regeneration then they should also possess the same properties as that of a tissue and therefore should be tested for their viscoelasticity.

Some of the basic phenomena experienced by viscoelastic materials are *i*) if stress is held constant, then strain increases with time (creep), *ii*) if strain is held constant, the stress decreases with time (relaxation), *iii*) effective stiffness depends on the rate of load and *iv*) in case of cyclic loading, hysteresis occurs [74].

Viscoelasticity is the property of a material that displays both viscous and elastic nature during deformation [75]. Deformation could be in forms of stretching, compressing or stretching and relaxing continuously at a constant or variable strain rates.

A normal elastic material has the ability to undergo deformation under high strains but can quickly come back to its original shape when the strain is removed. This is due to the bonding of the material where the linking is stretchable within a limit. A popular model for many elastic materials is Hooke's Law, which is based on the linear relationship of stress and strain. For an elastic material Hooke's Law is give by:

$$\sigma (\text{Tensile Stress}) = E(\text{Modulus of elasticity}) \times \epsilon(\text{Strain})$$

In a viscoelastic material, its properties and microstructure allow it to come back to its original shape after a certain time and hence show time dependent strain behavior [75]. The stress-strain behaviors of elastic and viscoelastic materials are shown in **Figure 6**. In figure 6a the elastic material shows linear behavior when a stress is applied and gets back to its original form in the same path it took to elongate itself under stress. On the other hand a viscoelastic material shows a nonlinear relationship between stress and strain and hence deviates from Hooke's law. It takes a different path to get back to its original form once the stress is released and takes a longer time due to the viscous component present in the material. Hence, it shows time dependent strain behavior

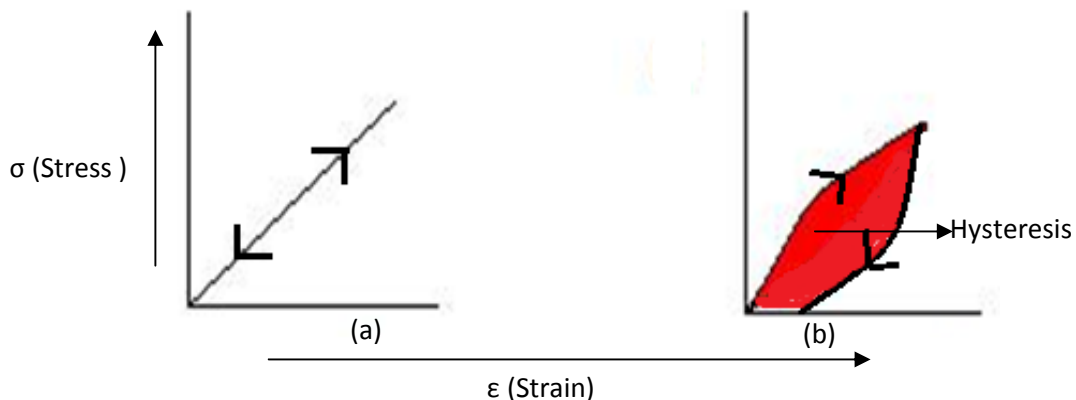


Figure 6: Stress-strain behaviors of (a) elastic and (b) viscoelastic materials during loading and unloading.

because stress increases much faster with increase strain than what Hooke's law predicts [76]. This variation in stress-strain behavior is due to the molecular structure of a viscoelastic material. Under stress these materials undergo some strain where in the molecular structure is disturbed but as the stress is removed they tend to come back to their original shape by re-arranging parts of their molecular structures and hence take a different path. Also during this molecular rearrangement known as, creep, there is some energy lost or dissipated by the material which is given by the area inside the loop [77-78]. This phenomenon is called hysteresis (Fig.2) and is not observed in elastic materials. The creeping effect of these materials gives them the viscous component and they get back to their original shape due to the elastic component, hence the name viscoelastic materials [78]. The stress-strain behavior of animal tissues deviates from Hooke's Law and so they behave as viscoelastic materials [79-83]. Also the presence of water in most of the body parts make these tissues behave like both solids and fluids or viscoelastic materials [84]. Therefore, the scaffold materials used in tissue engineering should also behave as viscoelastic materials.

In this study, chitosan and chitosan-gelatin are tested for their viscoelasticity. Usually elastic behavior is defined by a stress-strain curve (independent of time) but in a viscoelastic material stress, strain and time are coupled. And hence, a viscoelastic material needs to be tested for its tensile strength, stress-relaxation behavior and cyclic behavior to identify all its basic phenomena [74].

Tensile Strength

Before testing any material one needs to know its limit to withstand deformation or tensile strength. It is necessary to know how long, in length, a viscoelastic material can be stretched before it breaks. So a tensile test is usually performed on a material to know its limit so that all other mechanical behaviors can be tested and observed below this limit. Any test beyond this limit will cause breaking of the material.

Tensile strength defines the maximum stress that a material can withstand. Tensile testing gives the behavior of a material when it is stretched at a constant rate until its break point is achieved. This break point is the maximum stress it can resist. Compressive strength also gives the limit of a material but the testing is done in the opposite direction to that of a tensile test. To know the compressive strength of a material, it is subjected to crushing and the point at which the sample gets crushed is the limit. Compressive strength is of importance when testing materials like bone and cartilage. But for most soft tissues, tensile testing is performed [85]. So in a uniaxial tensile testing stress and strain are simultaneously measured as a sample is grasped at two ends and pulled at a certain load rate. General tensile behavior of a material is demonstrated by a stress-strain curve as shown in **Figure 7**. The point at which it breaks is its maximum stress point or the break point. In case of an elastic material the material will return to its original shape when the stress is released, as long as it is in the elastic region. But in the plastic region, whatever material it may be, it does not break but will not return to its original form after the stress is released. A general stress-strain curve for a viscoelastic material is as shown in Fig.2.

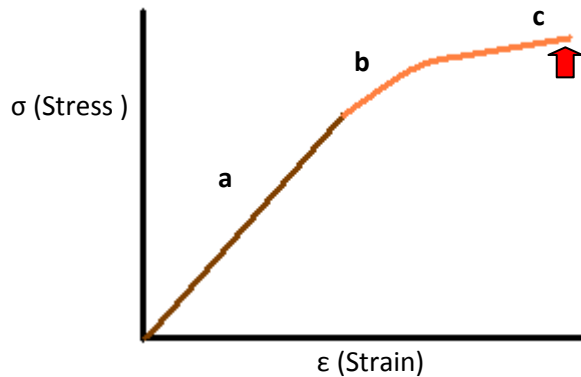


Figure 7: General stress-strain or tensile behavior of a material showing (a) elastic region, (b) plastic region and (c) failure.

Stress-Relaxation Behavior

Stress-relaxation behavior of a material gives important information of the scaffold on how it will perform during sudden application of stress as it is pulled (ramp) at a constant strain rate and is held at that rate for some time (hold), like in weight lifting and exercising.

When an external load is applied on viscoelastic materials, as the polymer is rearranging its chain a back stress is developed in the material. And these accumulated back stresses cause the polymer to return to its original form. At a constant strain the stress decreases with time and is called relaxation. This is a property of stress-relaxation is studied using a stress-relaxation (Ramp and Hold) test. So when a sudden constant load is applied to a viscoelastic material the initial stresses may be very high but with time the material relaxes to a steady state value of stress [78, 86]. This is due to accommodation of

the material to the induced deformation. So the variation of stress and its relaxation with time or strain at a constant strain rate is measured using the stress-relaxation test.

Cyclic Behavior

A scaffold needs to be tested for its performance during continuous or repetitive activities like walking and running. This performance under repetitive loading and unloading (cyclic loading) is the cyclic behavior of the material and it is tested by performing a cyclic test. In this test a cyclic stress is induced into the material by continuous pulling and relaxing of the material between a pre-defined lower and upper limit of load. The stress-strain curves during cyclic loading and unloading are different due to the viscoelastic behavior of the material (Hysteresis). These curves vary in dimensions as the number of cycles increase. Knowing the cyclic behavior gives us important information about the material properties and its applications [87].

Viscoelastic Models

Knowing how tissues in the body function is crucial to develop models which make estimation of their performances during stress and strain easier and can be used in many applications like injury prevention in automobiles, earplugs, sports, etc. When a tissue is being replaced by an external scaffold for tissue regeneration, then understanding the viscoelastic behavior of the scaffold material is also necessary to know how it performs during various applications. And modeling this material's experimental viscoelastic behavior can help in monitoring the changes in the stress-strain behavior of the scaffold that is placed in the body.

Tissues have a complex mechanical behavior and significant research has been done to develop models for the same [28-31]. As elastic materials obey Hooke's law, viscous fluids under shear stress obeys $\sigma = \eta \frac{d\varepsilon}{dt}$ [28].

There have been attempts in modeling the viscoelastic behavior by combining Hookean elastic elements and Newtonian viscous elements but for complex materials like tissues it is not possible to extract independent constants describing their viscous and elastic behavior [76]. One or more spring and dashpot models developed by Maxwell, Voigt and Kelvin (differential type) and Boltzmann model (integral type) were also used. These models have been further modified to suit the complex nature of tissues by arranging in various series and parallel networks [85]. But, these linear viscoelastic models did not account for nonlinear behavior of many soft tissues [84]. The most commonly used is the Quasi Linear Viscoelastic (QLV) model introduced by Y. Fung [28] was the first one to account for this deficit [84]. The QLV model describes the stress response of a material as a function of history and time [28, 88]. But, this model fails to predict the viscous responses, cyclic behavior and some of the complex strain-dependent relaxation of the materials. In addition to monitoring the stress-strain behavior, the model should also be able to convert the stress-relaxation data into cyclic behavior and convert the strain response to the stress response, etc. Different biological materials behave differently. So knowing the responses of each of them are necessary so that a universal model can be developed that suit their different complex natures [74]. On the whole the model should mimic the properties of the material being modeled.

To account for the *i*) stress-relaxation with time under a constant strain rate, *ii*) the deformation of the material shape under constant, *iii*) the gradual return of the material to

its original form once the load is released, *iv*) effect of cells, matrix, etc. on tissues and *v*) their inconsistent tissue properties; time-dependent, nonlinear, multi-component viscoelastic models are essential.

CHAPTER III

METHODOLOGY

MATERIALS AND METHODS

Materials

Low molecular weight chitosan ($M_n=80,000$), gelatin type A (300 bloom) and 500 kDa DS (contains 0.5-2.0% phosphate buffer salts) were purchased from Sigma (St. Louis, MO). Ethanol and hydrochloric acid were purchased from EM Science (Gibbstown, NJ) and Pharmco (Brookfield, CT), respectively.

Fabrication of Scaffolds

Chitosan solution with concentration of 2 wt% and 0.5 wt% were prepared in 0.06M hydrochloric acid. For chitosan-gelatin solution, similar amounts of gelatin were added to the chitosan solution. Both chitosan and chitosan-gelatin solutions were casted into rectangular or circular shapes on Teflon sheets, shapes created using silicone glue (**Figure 8**). Scaffolds (~4-mm thickness) were prepared by first freezing the respective solution at -80°C overnight and then lyophilized overnight (Virtis, Gardiner, NY). The porosity and pore size distribution of these matrices in hydrated condition has been extensively characterized and reported [20].

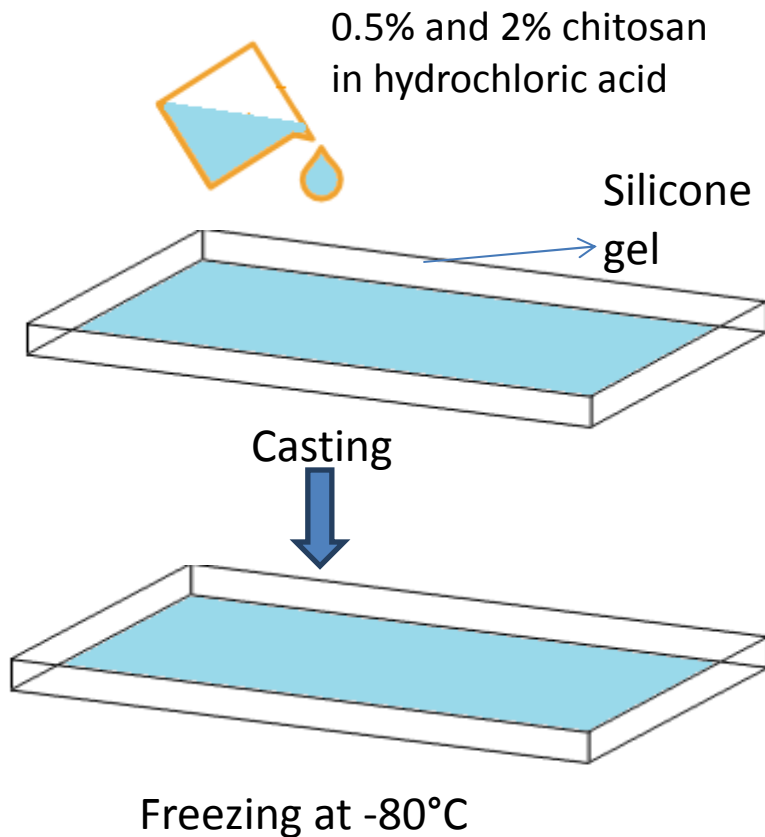


Figure 8: Solvent Casting of chitosan scaffolds using hydrochloric acid and freezing.

Mechanical Testing

The scaffolds were cut into 45mm long and 10mm wide rectangular strips, washed with ethanol and DI water to remove hydrochloric acid from the samples. All mechanical tests were conducted on an INSTRON 5542 machine (INSTRON, Canton, MA) on these rectangular strips of both chitosan and chitosan-gelatin scaffolds. Using the associated Merlin (INSTRON) software, data were recorded. All tests were performed under physiological conditions (hydrated in PBS at 37°C). On all tests minimum of four experiments were performed for each condition from different sample preparation. And the tests were run until we got at least four continuous and consistent

results. But only the best representative result for each test is shown in all the figures.

a) *Tensile testing.* Scaffolds were strained to break at 0.17mm/s (10 mm/min) crosshead speed, similar to previous reports [89].

b) *Stress relaxation.* For evaluating the stress-relaxation behavior of the scaffolds, five successive ramp and hold experiments were performed. All scaffolds were subjected to a constant step tensile strain applied at the rate of 2.5 %/s for 2 s followed by 58 s relaxation. The strain limit was fixed to 5% per ramp based on the load limits determined from the tensile behavior of chitosan scaffolds. To better compare the behaviors of chitosan and chitosan-gelatin scaffolds, the strain limit and rate of loading were kept constant for stress relaxation tests for both scaffolds (0.5wt % and 2wt %).

c) *Cyclical testing.* Scaffolds were also tested by cyclic conditions. Under cyclical loading, the strain rate was kept constant at 2.5 %/s, similar to stress relaxation experiments. Samples were stretched and reverted toward the original length repeatedly between two preset loads for five cycles. The load limits were selected based on the tensile property results and same limits were used to generate cyclical behavior from the stress relaxation data. The lower limit was set to 0.4KPa and upper limit was set to 1.4KPa. Additional cyclical experiments were performed with the same load limits but using a cross-head speed of 0.0867 %/s (5 mm/min) to evaluate the model predictions at a different strain rate.

Microstructure Characterization

To develop a model based on the physical changes in the scaffold, changes in the microstructures of the scaffolds before and after ramp and hold experiments were evaluated. For this purpose, the microstructures of chitosan and chitosan-gelatin

scaffolds were analyzed using an inverted microscope (Nikon Eclipse TE2000U, Melville, NY) in hydrated condition. Scaffolds were hydrated in Phosphate Buffer Saline (PBS) and aligned in the direction of pull. Digital micrographs were captured and analyzed for changes in the fiber orientation. The changes in microstructures before and after stress-relaxation tests for chitosan and chitosan-gelatin are shown in Figure 1. The direction of their stretching and orientation of the scaffolds was the same and is indicated by arrows in **Figure 9**.

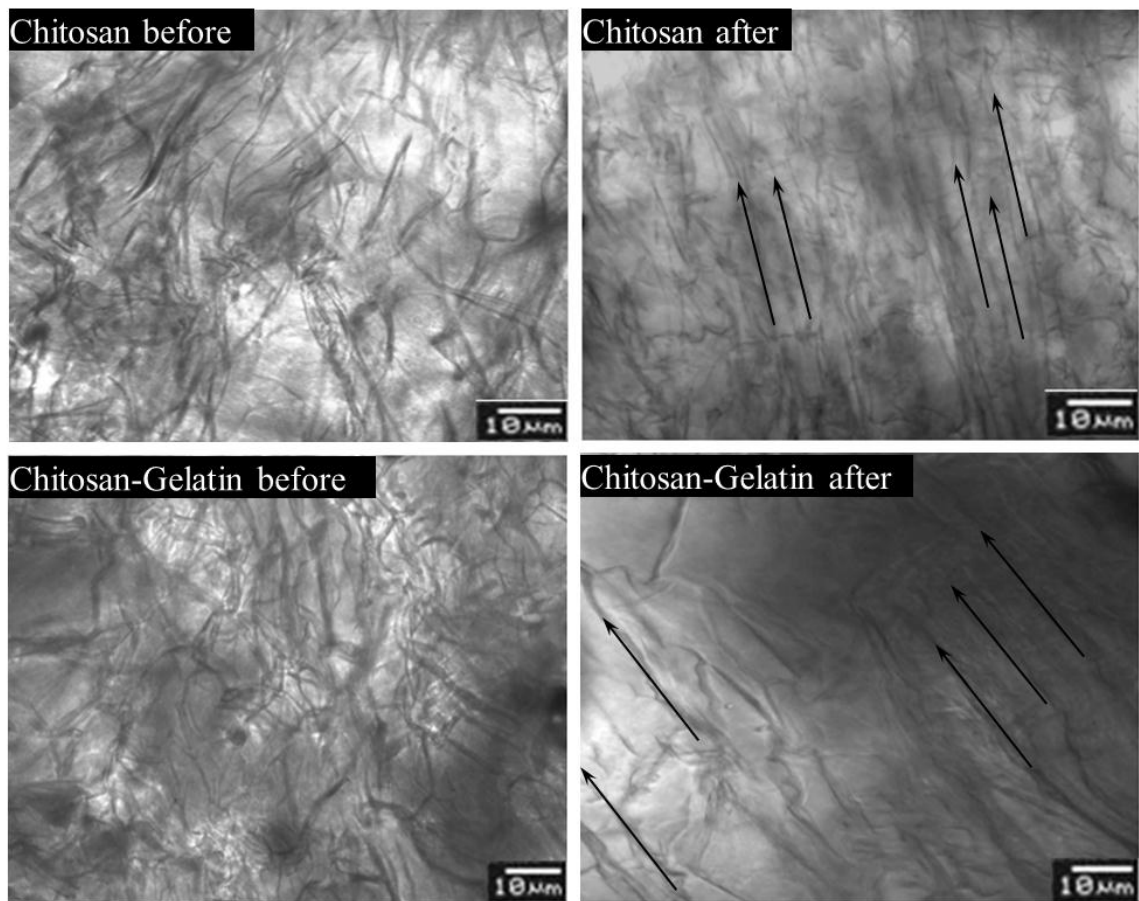


Figure 9: Micrographs of scaffolds showing porous structure before and after ramp and hold experiment.

MODELLING

Pseudo-Component Models.

Time-dependent (viscoelastic) models are required since the scaffold stress relaxes in time under constant strain, and the tissue shape progressively deforms under constant load. The time-dependent behavior also depends on the stress-strain history. Further, nonlinear, multi-component, viscoelastic models are required since scaffold properties are not constant. Finally, since many scaffold components do not relax fully to the original internal structure, the commonly employed dashpot element (which assumes the spring return to zero stress) is not appropriate. For this purpose, new constitutive relations based on pseudo-components were developed for the nonlinear, multi-component, viscoelastic behavior of chitosan and chitosan-gelatin scaffolds. These are described below.

Pseudo-component 1: Hyper-elastic spring: This component characterizes the material in such a way that it does not relax internal stress and the material rebounds to its original structure and size on removal of external load. The hyper-elastic spring component has a stress response to the strain that is nonlinear as shown in **Figure 10 Curve a or b.**

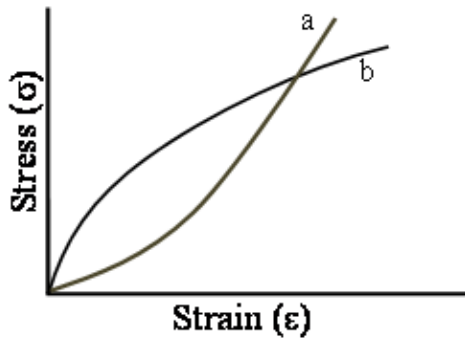


Figure 10: Schematic interpretation of Non-linear response of stress with increase in strain

Pseudo-component 2: Retain component: The microstructure of both chitosan and chitosan-gelatin scaffolds were observed under an inverted microscope before and after a stress-relaxation test. These results (**Figure 9**) showed a random distribution of features (revealed as lines, defects, or shadows) prior to stretching. After strain, and some relaxation at the stretched condition, then strain relief, scaffolds from both materials showed a general orientation of the features, which are aligned along the direction of pull. This suggests that the scaffolds retained certain structure acquired during loading. By contrast, a spring and dashpot model describes a material that returns to its original relaxed structure when held under strain. Upon subsequent strain, a spring and dashpot model reinitiates its stress-strain relation at the origin of **Figure 10**– the increase in stress response to strain is characteristic of the origin. Observations from **Figure 9** reveal that the underlying structural features are retained while the scaffold is allowed to relax under strain. This suggests that the stress response from a subsequent strain starts

with the oriented structure – the increase in stress response to strain is characterized by the slope at the strained point. To account for the nature of the material to retain components were added in parallel to the hyper-elastic spring model as indicated in **Figure 11**.

Two types of composite models were investigated.

5-parameter Model –one hyper elastic spring component in parallel with one retain pseudo-component (as illustrated in Figure 11a).

8-parameter Model – This structure had one hyper elastic spring component in parallel with two retain pseudo-components (as illustrated in Figure 11b).

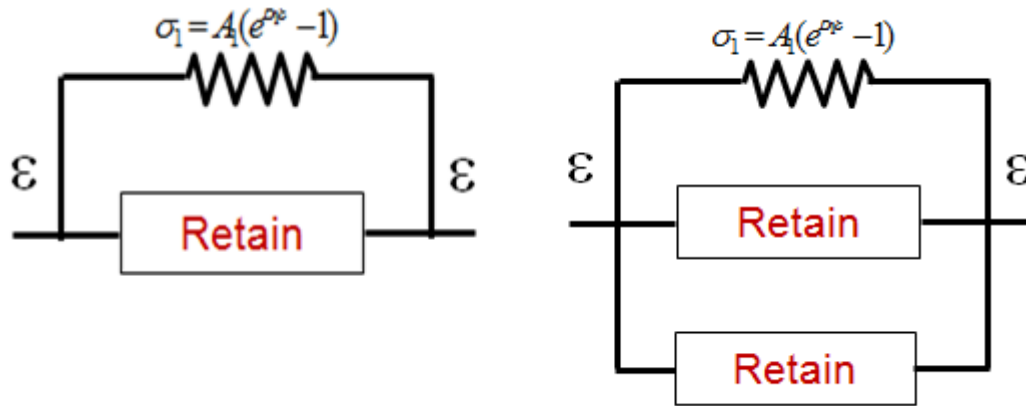


Figure 11: Model with (a) one hyper elastic spring and a retain pseudo-components
(b) one hyperelastic spring and two retain pseudo-components in parallel.

Mathematical Statement.

Figure 11a symbolizes for a pseudo-component an instantaneous nonlinear stress-strain relation modeled as,

$$\sigma_i = A_i \left(e^{B_i \epsilon_i} - 1 \right) \quad (1)$$

where “i” (subscript) represents the i^{th} pseudo-component. In this equation the coefficients A and B should have the same sign. Curve a and curve b in **Figure 10** illustrates the plot when $A, B < 0$ and $A, B > 0$ respectively.

Each pseudo-component undergoing internal material deformation was modeled to have a first-order rate of internal stress relaxation, which relaxes rapidly initially and asymptotically to zero stress. The relaxation model with no strain-rate-induced stress is a first-order ordinary differential equation, written as

$$\tau_i \frac{d\sigma_i}{dt} + \sigma_i = 0, \quad \sigma_i(t=0) = \sigma_0 \quad (2)$$

For the material with internal deformation concept (**Figure 11**), Equation (1) is the stress model when instantaneous strain at one stage is applied, stress relaxation is revealed by Equation (2) if for a period of time the elongation is held then. However, when the material is relaxing after strained at a particular rate, then derivations done rigorously enumerate that Equation (2) should include the injection of internal stress at that particular rate. The retain part which allows a stress relief can be written as

$$\tau_i \frac{d\sigma_i}{dt} + \sigma_i = \tau_i \frac{\partial \hat{\sigma}_i}{\partial \varepsilon} \frac{d\varepsilon_i}{dt} = \tau_i A_i B_i \exp(B_i \varepsilon) \frac{d\varepsilon_i}{dt}, \quad \sigma_i(t=0) = \sigma_0 \quad (3)$$

Thus, given the stress of pseudo-component “i” which is partially relaxed, at the completion of a Δt time increment, the strain equivalent on the strain component can be determined by the inverse of Equation (1)

$$\varepsilon_{equ,i}(t + \Delta t) = \ln \left(\frac{\sigma_i(t + \Delta t)}{A_i} + 1 \right) / B_i \quad (4)$$

Equation (4) gives the value of equivalent strain from which for a pseudo-component the equivalent length is the length that the material would shrink back to when all stress be

removed. Because the component will have been deformed, it will not shrink back to its original length. L_{equ} is calculated as

$$L_{equ,i}(t + \Delta t) = L_0(1 + \varepsilon_i(t + \Delta t)) \quad (5)$$

The sample length at the next time instant, t , can be calculated from experimental strain, ε_0 as

$$L(t) = L_0(1 + \varepsilon_0(t)) \quad (6)$$

and hence the new strain that is effective on the pseudo-component is

$$\varepsilon_i(t) = \frac{[L(t) - L_{equ,i}(t)]}{L_{equ,i}(t)} \quad (7)$$

For each pseudo-component the stress vs. time is modeled by sequential application of Equations (6), (7), (3), (4) and then (5). As numerical methods are used to solve equations Δt should be small relative to the time-constants and the time periods taken for the corresponding changes in strain rate. Here, the measurement during experiment in a tensile test is tensile force but the tensile tests report stress. The tensile force obtained here is represented as the sum of all forces attributed to each of the pseudo-components.

Assuming that each of the pseudo-components retain a volume that is constant upon deformation, and the contraction in each of the dimensions is uniform, and the length of the material L is long enough that the geometric end effects due to the clamping of the sample could be eliminated, the extension in length due to strain causes the cross-sectional area to reduce to as

$$A = \frac{A_0}{(1 + \varepsilon_0)} \quad (8)$$

If for a i^{th} pseudo-component having a representation as Equation (3) and if it is relaxed to the equivalent length, the “original” area that is unstressed is

$$A_i = \frac{A_0(1 + \varepsilon_i)}{(1 + \varepsilon_0)} \quad (9)$$

Hence the force due to the stress on i^{th} pseudo-component of Equation (3a) will be,

$$F_i = \sigma_i A_i = \frac{\sigma_i A_0 (1 + \varepsilon_i)}{(1 + \varepsilon_0)} \quad (10)$$

The measured stress is determined by volume weighting, by ϕ_i , the volume fraction, ratio of sum of the forces due to each of the pseudo-components to the original area A_0 ,

$$\sigma_{\text{Composite}}(t) = \sum_{i=1}^N \frac{\phi_i \sigma_i(t) (1 + \varepsilon_i(t))}{(1 + \varepsilon_0(t))} \quad (11)$$

Where, “N” stands for the total number of pseudo-components. For the fluid rearrangement components, internal volume does not remain constant and there is no material deformation, making $\varepsilon_i = \varepsilon_0$.

It would seem that the volume fraction, ϕ_i , and the stress-amplitude factor, A_i , from Equation (1) are independent model parameters. However, when Equation (11) is written in terms of strain only, the two coefficients appear as a product.

$$\sigma_{\text{Composite}}(t) = \sum_{i=1}^N \frac{\phi_i A_i (e^{B_i \varepsilon_i(t)} - 1) (1 + \varepsilon_i(t))}{(1 + \varepsilon_0(t))} \quad (12)$$

Experimental stress-strain-time data cannot separate the functionality of ϕ_i and A_i . Accordingly, the model coefficients that characterize the viscoelastic properties of each pseudo-component that are adjustable in the “AB” material will be the ϕA_i product, B_i , and τ_i . If the pseudo-components are identified and volume fractions are known, then τ_i , A_i , and B_i would be the adjustable model coefficients. However, the pseudo-component

is not meant to represent one particular component, but the collective behavior of the integrated whole. This work will propose τ_i , the ϕA_i product, and B_i as adjustable model coefficients.

At each time step, Δt , Equation (11) provides the value of the superficial stress measured on the composite. One major asset of this time-incremental, numerical model vs. analytical integrated model is that for the time-dependent behavior rate of strain there are no assumptions. The computational algorithm is not changed even when the strain rate is started, stopped, changed, or re-started. Further, it is a simple task to replace the instantaneous stress-strain relation of Equation (1) and its inverse of Equation (4) with another relation. In order to determine values of the model parameters that is adjustable least squares regression using $\sigma(t)$ and $\varepsilon(t)$ data and the pseudo-component model that is numerically-solved to predict the measured stress of the composite models will be used.

Based on these mathematical statements, codes were written in Visual Basic for Applications with an interface in Excel. The objective function was defined as the summation of square of the difference (SSD) of the experimentally determined value to the analytically obtained value from the equation of stress. The SSD was calculated both for the loading as well as the relaxation part of the experimental data and represented mathematically as

$$SSD = \sum \left(\sigma_{\text{model data}} - \sigma_{\text{experimental data}} \right)^2 \quad (13)$$

Random initial guesses were generated for the model parameters by the optimizer. As typical of nonlinear optimization there can be local minima that attract the optimizer. To find the global best solution the optimizer was run from N independent initializations. “Best-of-N” analysis developed by Rhinehart and Iyer [90], where N is the number of

independent optimizations. The value of N is designed to probably find one of the best of all possible objective function values, and is calculated using

$$N = \frac{\ln(1 - P_{\text{success}})}{\ln(1 - f_{\text{best}})} \quad (14)$$

Where, P_{success} is the user-desired probability that the best from N will yield a SSE value which is one within the best fraction, f_{best} , of all possible values. In this work, 22 iterations were used based on the desire to find one of the best 10% of all possible objective function values at least once with 90% confidence.

$$N = \frac{\ln(1 - 0.90)}{\ln(1 - 0.10)} = 21.85 \cong 22$$

Out of the N results obtained, the run with the minimum SSE value was chosen as the resulting value for the model parameters. The stress-relaxation behavior of both chitosan and chitosan-gelatin were fitted using 5-parameter Model and 8-parameter Model and were compared to choose the best model. The parameters of model that is chosen should mimic the properties of scaffold. The model chosen should be able to fit the stress-relaxation data and predict their cyclic properties.

CHAPTER IV

RESULTS

Tensile Testing

Previous results show that blending gelatin to chitosan does not significantly alter the porous architecture of the scaffolds [91]. To confirm this, some of the scaffolds were observed under scanning electron microscope (data not shown) to confirm the behavior. Next, uniaxial tensile testing of chitosan under physiological conditions revealed a non-linear tensile behavior even at small strain ranges. Further, 0.5 % (wt/v) of chitosan scaffolds stretched up to 25-30% of their original length before failure (**Figure 12**) at 3 KPa stress. With the addition of gelatin and increase in chitosan concentration, scaffold strength increased. All other tests that were conducted used an upper limit of 3 KPa for better comparison. From the break strain, limit of strain per ramp was calculated to be 5% and the samples were stretched at a strain rate of 2.5 %/s.

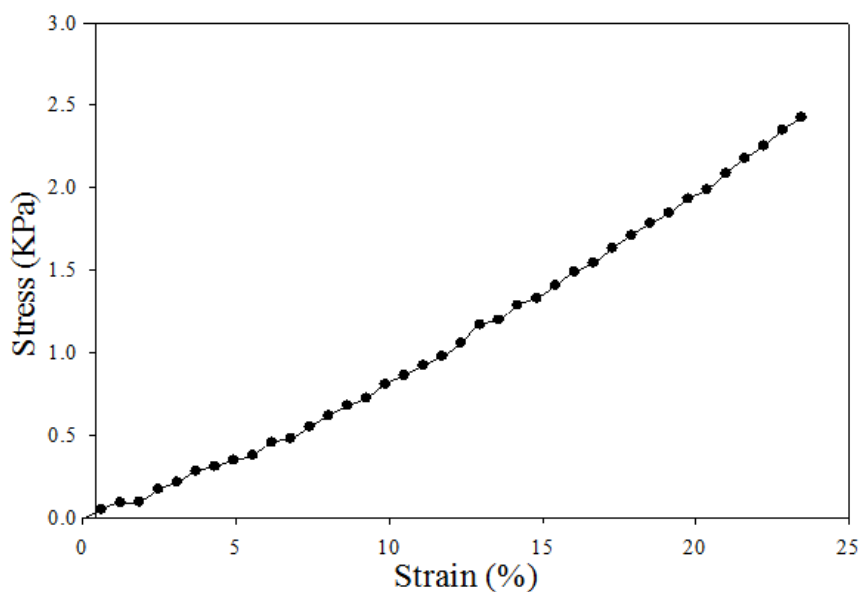


Figure 12: Stress-strain behavior of scaffolds in hydrated conditions.

Stress-Relaxation Behavior

To compare the stress-relaxation behavior of chitosan and chitosan-gelatin “ramp and hold” tests were performed. These results (**Figure 13**) showed that the stress-relaxation behaviors of chitosan and chitosan-gelatin were similar. Both showed a progressive increase in their stress values but 2 wt% chitosan withstood stress up to 8 KPa and (2 wt%-2 wt%) chitosan-gelatin scaffold withstood stress up to 11 KPa. The stress relaxation behavior of 0.5 wt% chitosan and 0.5 wt%-0.5 wt% chitosan-gelatin was also similar but the former withstood a stress up to 2.2 KPa and the latter withstood a stress up to 4.5 KPa, which suggested an increase in stress limit due the addition of gelatin. This also validates the method of testing stress-relaxation behavior as chitosan and chitosan-gelatin are stronger at a concentration of 2 wt% than at 0.5 wt%.

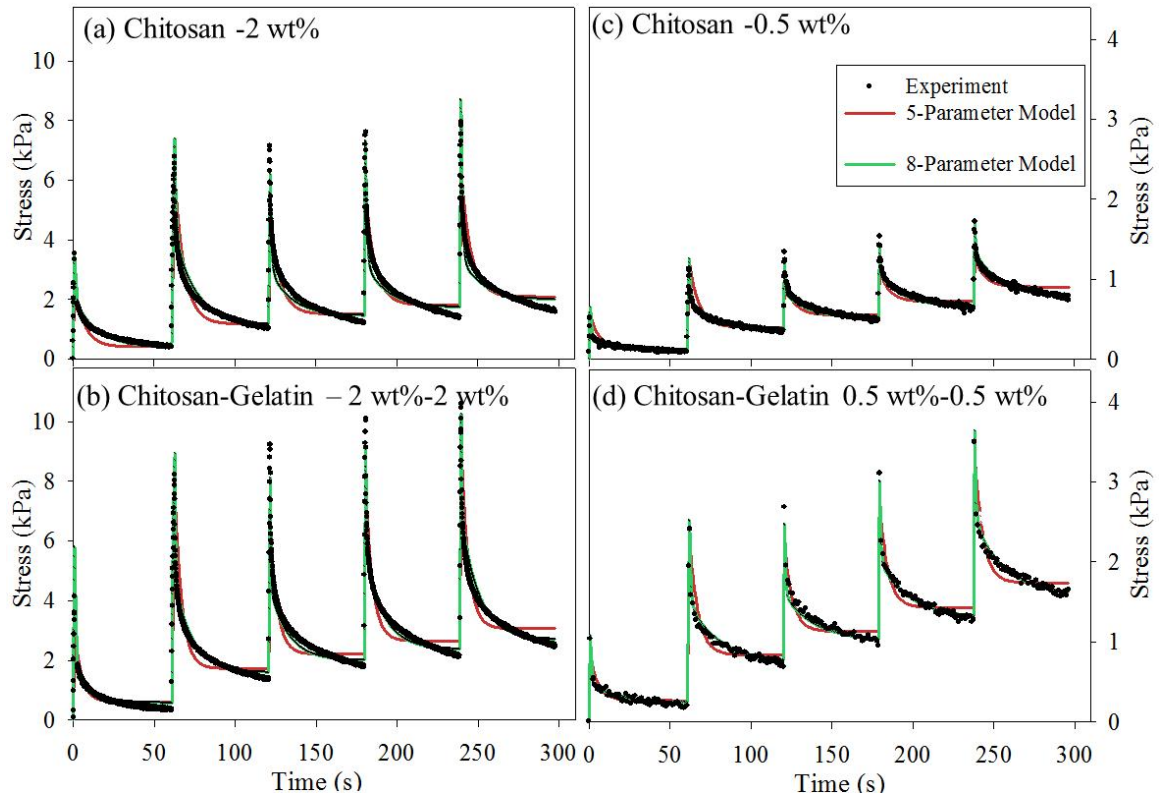


Figure 13: Dynamic behavior of different scaffolds and comparison of model predictions to representative experimental result ($n=4$).

Since different levels of maximum stresses were observed between different samples, relaxation stresses were plotted by normalizing the data in the first stage to the highest stress experienced by the scaffold (**Figure 14**). This was referred as the normalized relaxation function, $G(t)$. These results showed that all scaffolds relaxed nearly 90% of their stresses when held for 60 seconds and the behaviors in all four conditions were similar. There was no significant difference in the relaxation behavior in the absence or presence of gelatin. In addition, the increased concentration of polymers did not affect the relaxation behavior.

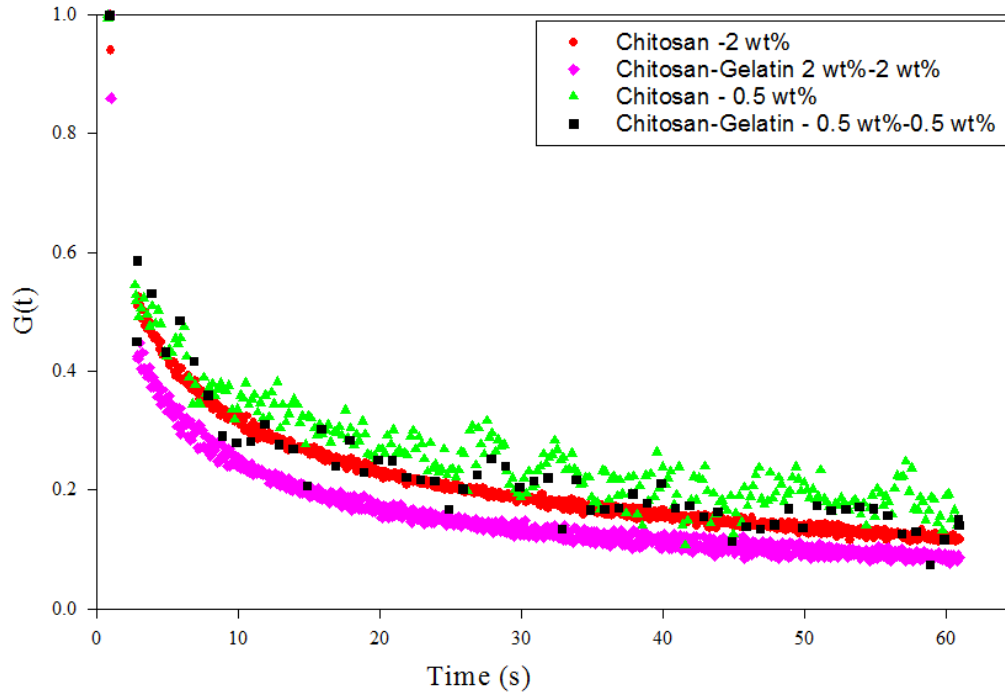


Figure 14: Stress relaxation function, $G(t)$, plot from the characteristic trend of the first cycle of each strain rate.

To understand the behavior of relaxation in subsequent cycles, all cycles were plotted by translating the stress pattern for each stage to the origin (**Figure 15**). There was no significant difference in all the stages in each sample and the stress relaxation ratio in each cycle was identical. This was unlike the relaxation characteristics observed for 50:50 poly-lactide-co-glycolide (PLGA) samples and small intestinal submucosa (SIS) matrixes under similar evaluation conditions [89].

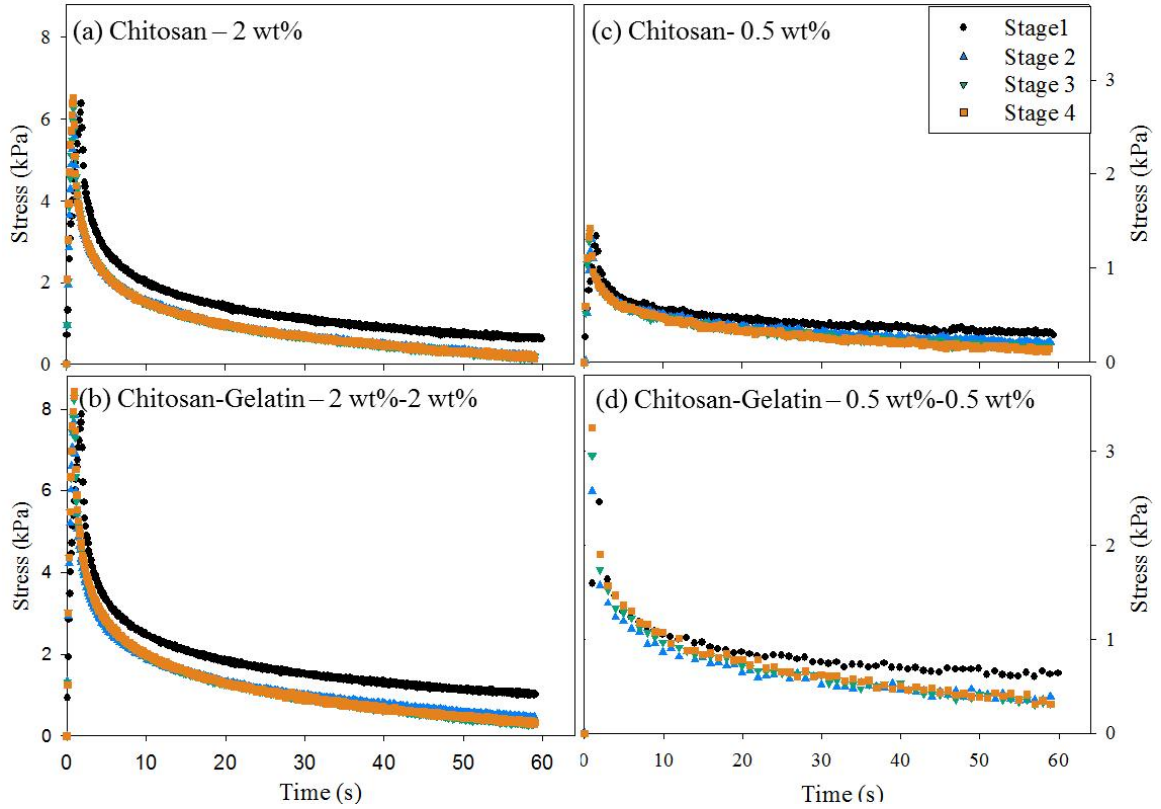


Figure 15: Relaxation behavior of scaffolds in different stages of ramp and hold tests. A representative result is shown for each test ($n=4$).

PLGA membranes showed a decrease in peak stresses in successive stages whereas SIS showed an increase in peak stress in successive stages. This difference is because of the difference in the micro-structures of both the polymers. 50:50 PLGA is an amorphous linear polymer whereas SIS is a natural matrix comprising of rich collagen type 1 and other matrix elements. Since chitosan is a linear polysaccharide matrix and during the formation of gelatin the collagen chains in gelatin are broken, both of them show difference in the stress-relaxation behavior. But chitosan scaffolds did show an increase in the peak stress due to its natural origin but not as drastic as that of SIS.

Model Parameter- Values.

Based on the microstructural changes in chitosan and chitosan-gelatin scaffolds, a composite pseudo-component model was developed. Both the ramp and the relaxation parts of the experimental results were simultaneously used to determine all parameters. First, *5-parameter model* (Figure 11a) consisting of one retain component and one hyper elastic spring was fitted with the experimental data as shown in figure 13.

| Parameters | Chito 0.5% | Chito-Gel 0.5% | Chito 2% | Chito-Gel 2% |
|------------------------|------------------------|------------------------|-----------------------|-----------------------|
| Ax1(Pa) | 0.974 | -4.28×10^4 | 1.20×10^4 | 3.75×10^3 |
| B1 | 2.856 | -1.78×10^{-4} | 1.74×10^{-3} | 3.43×10^{-3} |
| Ax2(Pa) | -3.70×10^6 | 0.859 | 19.470 | 12.1 |
| B2 | -3.69×10^{-6} | 8.07 | 3.939 | 4.20 |
| Tau2(s) | 5.01 | 5.28 | 5.950 | 4.38 |
| SSD(KPa ²) | 14.8 | 13.9 | 1.22E+03 | 575 |

Table 1: Parameter and SSD values of 5-parameter Model.

The model converged (**Table-1**) and gave parametric values with SSDs of 1216.71 KPa² and 574.90 KPa² for 2 wt% chitosan and (2 wt%-2 wt%) chitosan-gelatin, respectively. Using the parameters determined from the analytical model, relaxation characteristics were predicted for different time points, which showed disagreements in the relaxation portion of the experimental data. The relaxation portion for each stage is when the stress value drops as strain increases (**Figure 13**). Similar behavior was observed for 0.5 wt% scaffolds. However, the SSDs were lower than that of 2 wt% scaffolds. In the case of 0.5 wt% chitosan scaffolds, data was fitted with a SSD of 15 KPa² and that of 0.5 wt%-0.5 wt% chitosan gelatin was 14 KPa². To understand the meaning of these parameters, product of A and B from each element were compared. These calculations showed that the product of A and B in both hyperelastic component

and the retain element were significantly higher for 2% scaffolds relative to 0.5% scaffolds. However, the time constants were comparable in all the samples.

To improve the model i.e., to reduce the SSD, another retain pseudo component was added to the 5-parameter model and tested for suitability. These results (**Figure 13**) showed that 8-parameters model fitted the stress-relaxation data of 2 wt% scaffolds with decreased SSDs of 273 for chitosan and 178 for chitosan-gelatin (**Table-2**).

| Parameters | Chito 0.5% | Chito-Gel 0.5% | Chito 2% | Chito-Gel 2% |
|------------------------|------------------------|-----------------------|-----------------|------------------------|
| Ax1(Pa) | 1.34 | 1.46 | 878 | -25.9 |
| B1 | 2.13 | 3.15 | 0.021 | -0.471 |
| Ax2(Pa) | -3.53×10^6 | 3.55 | 75.0 | -1.47×10^6 |
| B2 | -8.77×10^{-5} | 4.95 | 2.42 | -1.40×10^{-4} |
| Tau2(s) | 0.022 | 0.696 | 0.547 | 0.436 |
| Ax3 (Pa) | 0.555 | 0.584 | 7.76 | 3.35 |
| B3 | 6.20 | 7.27 | 4.87 | 5.88 |
| Tau3(s) | 10.4 | 14.2 | 13.4 | 11.0 |
| SSD(KPa ²) | 4.61 | 4.03 | 273 | 178 |

Table 2: Parameter and SSD values of 8-parameter Model.

These numbers were much lower than those of 5-paramters model although higher than that of 0.5 wt % scaffolds. Importantly, relaxation characteristics determined from the parameters showed agreements in the relaxation portion of the experimental data. To understand the meaning of the parameters, product of A and B from each element were compared. These calculations showed that the product of A and B in the hyperelastic component and one of the retain component were significantly higher for 2% scaffolds relative to 0.5% scaffolds. However, the product of A and B were similar in the other retain component. With respect to time constants, they were not significantly different between different scaffold preparations. However, one time constant was significantly less than the second time constant in the same scaffold; one time constant

was less than one second while the other was more than ten seconds. The average of these time constants was similar to the single time-constant value of the 5-parameter model. Thus the addition of second retain component segregated the fast relaxation components from slow relaxation components within each scaffold. This suggested that the chitosan and chitosan-gelatin scaffolds are composed of both fast and slow relaxation elements and the need to include two retain components to predict time-dependent behavior of chitosan and chitosan-gelatin structures.

Cyclic Behavior

Regular activities like walking, lifting weights, cycling, and all those have a controlled repetitive stresses on muscle fall into this category of testing. Apart from the viscoelastic models, typically cyclical experiments are conducted separately to assess the fatigue characteristics. We questioned whether the developed pseudo-component model parameters could be used to predict cyclical behavior of porous scaffolds. The data were generated using various increments of stress between the 0.4 KPa and 1.4 KPa and predicting the strain values using parameters from the 8-parameter model for respective scaffolds. The limits for the cyclic behavior were chosen based on the tensile properties of chitosan.

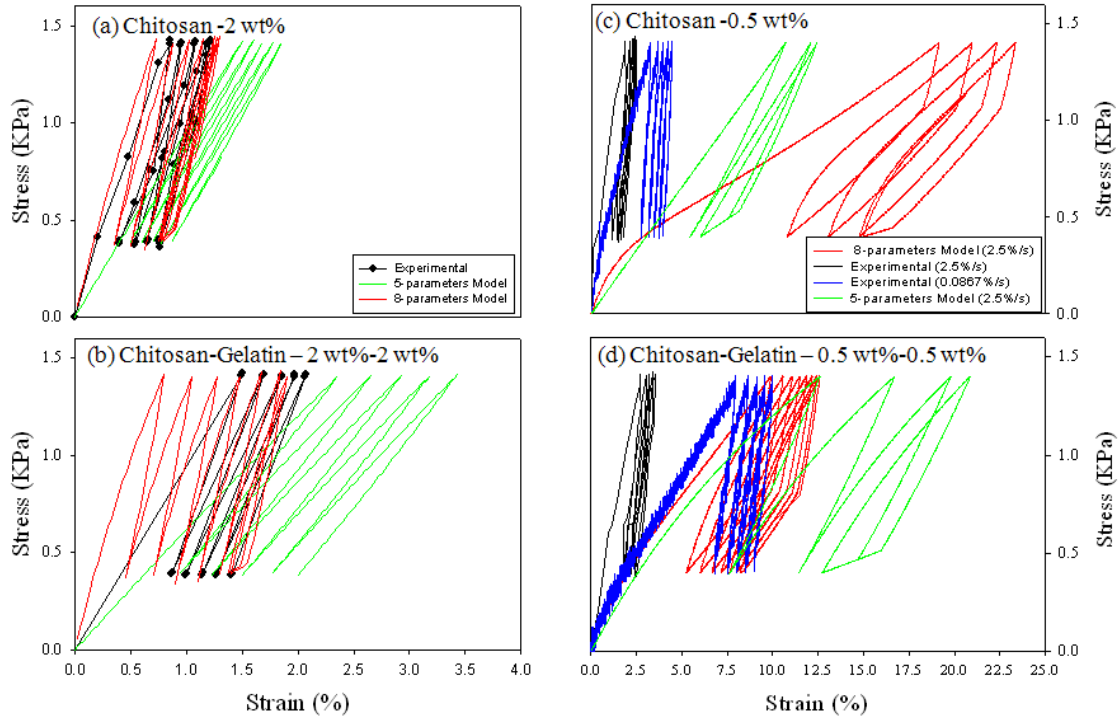


Figure 16: Cyclic behavior of different scaffolds and comparison of model predictions.

The 2 wt% chitosan cyclic behavior was predicted as withstanding a strain up to 1.2% (as illustrated in **Figure 16a**). For 2 wt%-2 wt% chitosan-gelatin the extension was predicted to be 2%. The 0.5 wt% chitosan cyclic behavior was predicted as withstanding a strain up to 20%. For chitosan-gelatin the extension was predicted to be 13%. So the cyclic predictions were generated using both the models for all scaffolds as shown in figure 16.

To validate these model predictions, chitosan and chitosan-gelatin were tested for their cyclic behavior between the same stress limits of 0.4 KPa -1.4 KPa at 2.5%/s. These results (**Figure 16(a,b)**) showed the cyclic region to be between 0.4% and 1.3% for 2 wt% chitosan and that of chitosan-gelatin was between 0.8% and 2% at a strain rate of 2.5 %/s, similar to the model predictions. The 5-parameter model was also used to

predict the cyclic data (**Figure 16**), which showed distinctly different results compared to the 8-parameter model for 2 wt% scaffolds, despite general agreement with experimental results. Hence, the 8-parameter model is a better choice than the 5-parameter model. The cyclic region of 0.5wt% chitosan at 2.5%/s was between 1% and 2.5% of strain and addition of 0.5 wt% gelatin shifted the cyclical region to 1% and 3.5% under same stress conditions. On the contrary to 2% chitosan results, the model predictions for 0.5 wt% scaffolds were significantly higher than the experimental results. The experimental data showed extension up to 2.5% for 0.5 wt% chitosan and 3.5% for 0.5 wt%-0.5 wt% chitosan-gelatin scaffolds. The predicted range of strains that the materials can withstand, at a given strain rate, was much higher than their experimental behavior of 0.5 wt% scaffolds.

This indicates that the model is predicting higher strains for lower concentration scaffolds than what they can actually withstand at a constant strain rate; nevertheless these predictions lie under the tensile limit of the materials. Model predictions were in agreement (**Figure 16a**) for the 2 wt% scaffolds under the same set of parameters but slight variations in the cyclic regions of the predicted and experimental cyclic behavior can be observed in 2 wt%-2 wt% chitosan-gelatin scaffold (**Figure 16b**). The model could accurately predict the cyclic behavior of scaffolds at higher concentration and not at lower concentration. This could be due to the random orientation of pores at a lower concentration and more oriented pores at higher concentration. Hence, given more information about the materials like polymer structure, molecular weight, porosity, etc. the model could predict the cyclic behaviors more accurately.

To understand the effect of strain rate, experiments were conducted on 0.5 wt%

scaffolds for cyclic behavior at strain rate of 0.0867%/s (5% per minute) under the same stress limits of 0.4 KPa and 1.4 KPa. Reduction in strain rate allowed 0.5 wt% chitosan and chitosan-gelatin to extend up to 4% and 8.5% (**Figure 16(c,d)**) of their lengths, respectively. Overall, the behavior of the scaffold did not change with change in the strain rate. As the strain rate was lowered the ability of the material to stretch increased. Irrespective of the strain rate and concentration, addition of gelatin added strength to the chitosan scaffolds. This suggests that addition of gelatin without cross linking does increase the strength of chitosan. The cyclic region of 0.5wt% chitosan at shifted to 2% and 4% at 0.0867%/s strain rate and that of 0.5wt%-0.5wt% chitosan-gelatin were between 6.5% and 8.5%. Although region of cyclic was greater for chitosan-gelatin than chitosan, hysteresis region of 0.5 wt% chitosan did not change much (**Figure 16c**) even with the change in strain rate. When the model was used to predict the cyclic behavior at a lower strain rate of 5% per minute, it could not predict. This was because the model reads the materials as already relaxing while stretching due to a very low rate. So little refining of the retain pseudo-components is necessary for a better prediction at lower strain rates.

CHAPTER V

DISCUSSION

This study explored the viscoelastic properties of chitosan and how these properties vary with the addition of gelatin to chitosan. Viscoelastic properties were evaluated via ramp and hold test to evaluate the stress relaxation behavior and used a pseudo-component model to describe the stress-strain properties of chitosan and chitosan-gelatin scaffolds in multiple strain stages. Also these properties were used to validate the presented model and checked if it was effective enough in predicting the properties of chitosan and chitosan-gelatin composite scaffold [16, 20, 92]. First, the tensile test results showed value of stress limit much less for chitosan and chitosan-gelatin scaffolds than other synthetic scaffolds like PCL [93], PLGA [89], human skin [94] and porcine bladder constructs [95]. These results are dependent on the molecular weight of chitosan with >310 kD MW had a greater range of stress carrying capacity without deformation relative to 50 to 190 kD chitosan used in this study [96]. Further, the initial segment of the tensile stress-strain curve showed non-linear relationship.

The stress relaxation behavior of chitosan scaffolds were different from 50:50 poly-lactide-co-glycolide (PLGA) scaffolds and also from small intestinal submucosa (SIS) [89]; the stress accumulation of PLGA matrix decreased in successive stages, the stress accumulation of SIS was increased in successive stages but chitosan and chitosan-

-gelatin scaffolds showed, no change in stress accumulation in successive stages. The difference in relaxation characteristics is attributed to the difference in the molecular properties of the polymers making the matrix: 50:50 PLGA is an amorphous linear polymer whereas SIS is a natural matrix with high amounts of type 1 collagen dispersed with other matrix elements. Chitosan is a linear polysaccharide harvested from a structural component of crustaceans and gelatin is denatured collagen. The polymer bonding between chitosan and gelatin is primary electrostatic rather than covalent bonds that would be observed in SIS. Chitosan scaffolds did show an increase in the peak stress due to its natural origin but not as drastic as that of SIS. These differences probably attribute to the observed differences in relaxation characteristics.

The initial segment of the tensile behavior is non-linear like a viscoelastic material. To account for the non-linear behavior of viscoelastic materials [97], a commonly used is the Quasi Linear Viscoelastic (QLV) model introduced by Y. Fung [28]. The QLV model describes the stress response of a material as a function of history and time [28, 98]. Since this model has many caveats, other approaches have been developed using numerical techniques as different biological materials behave differently [99-100]. The model should mimic the properties of the material being modeled, for which knowing the responses under various loading conditions are necessary to integrate their complex natures [101]. Delphine et al [102] in order to fit their experimental stress relaxation data of enzymatically digested bovine annulus fibrosus and nucleus pulposus tissue used a biphasic model with strain-dependent permeability and nonlinear elasticity. The model assumed the material as a permeable and porous solid matrix having inviscid interstitial fluid. The model considered that the viscoelastic effects were attributed to

momentum exchange between the fluid and solid phases caused due to frictional drag. Li and Herzog [103] did a numerical formulation for the role of viscoelasticity of collagen fibers in articular cartilage. They modeled the collagen matrix of articular cartilage as viscoelastic material using a QLV formulation having strain dependent elastic modulus. They modeled the proteoglycan matrix as linearly elastic.

Since the model should mimic the properties of the material being modeled, knowing their responses are necessary to integrate their complex natures [101]. Based on the deformation and their retention of new aligned structures observed in the microstructures of chitosan and chitosan-gelatin, a model was developed. The model is a combination of hyper elastic spring component and a retain component connected in parallel. The parameters generated by fitting the experimental stress relaxation data were used to predict the cyclical properties of the respective sample. These parameters define the properties of the respective sample, despite inconsistency in the values for chitosan and chitosan gelatin of the same concentration and different concentration too. 5-parameters model which has one retain pseudo component was successful in predicting the cyclical patterns of the materials irrespective of the high SSDs. There was, however, some variation in the predictions when compared to the accuracy of 8-parameters model. Having two retain pseudo components in the model gave better predictions. Similar methodology could be applied to other materials like synthetic polymers (PCL, PLGA) or other natural polymers (SIS, collagen), which may behave differently during stress-relaxation tests. The polymers might reform to their original structures after stretching and relaxation or part of the structure may reform and part of it may retain the deformations. So these can be accounted by adding just reform or both retain and reform

pseudo components to the model. One can use the common spring and dashpot component in parallel with other pseudo-components. Hence, different combinations of pseudo-components can be considered to model experimental data [104-105]. These might prove to fit the stress-relaxation data with lower SSDs.

The model could predict the cyclic behavior of scaffolds at higher concentration and the pattern of cyclic behavior at lower concentration, there was a disagreement in the estimated cyclical behavior of the materials at a lower concentration at a given strain rate. These discrepancies could be attributed to multiple factors i) variation in porous architecture at lower concentrations, ii) experimental methodology difference, and iii) consideration of five ramp-hold cycles for parameter determination. Improved methods should be used to produce low concentration scaffolds with consistent porous structures. The model was developed on the basis of stretching and relaxing of the scaffolds but the cyclical tests were conducted by continuous cycling of the samples, without allowing the samples to relax. So the variations in cyclical predictions can probably be minimized if the cyclic tests and predictions were based on cyclical stretch and hold basis with the same hold time used in stress-relaxation test. The model generates the cyclic and stress-relaxation data based on one strain period and one relax period only. The rest of the stages are derived analytically within the model. Also the number of model parameters required to fit the data was 8 which is the required number of parameters for the analytical models to model one strain and hold phase.

Researchers report difficulty in optimizing viscoelastic model parameter values to best match the model with experimental stress-strain-time data. There are multiple local optima, and approaches to the minima are often exasperatingly slow (even with classic

best practice nonlinear optimizers such as Levenberg Marquardt). Further, optimization must include constraints on the parameter values, suggesting that direct search methods may be more appropriate than gradient based methods. A new optimization technique called Leapfrogging was used [106]. Test cases on this technique revealed that this technique gave better optimized values when compared to other techniques with fewer number of function evaluations [106]. Accordingly, techniques such as best-of-N starts or direct search techniques have been investigated for determining the probable global optimum subject to multiple constraints. The applicability of emerging optimization techniques for model parameter adjustment is explored along with new regression approaches and the quality of the model.

CHAPTER VI

CONCLUSION AND FUTURE SCOPE

Conclusions

1. The stress relaxation properties of both chitosan and chitosan gelatin were similar except that chitosan-gelatin could withstand higher stresses and hence shows addition of gelatin makes chitosan stronger.
2. The relaxation properties for chitosan and chitosan-gelatin were similar.
3. Microscopic analysis of both scaffolds showed the retention of deformation when stretched and hence a model with hyper-elastic and retain pseudo-components were developed.
4. The 8-parameter model (one hyper-elastic spring and two retain pseudo-components) gave a better fit to the stress-relaxation data of the scaffolds than the 5-parameter model (one hyper-elastic spring and one retain pseudo-components) with lower SSD values.
5. The same 8-parameter model predicted the cyclic behavior of scaffolds at a higher concentration (2wt %) but showed variations in predicting the cyclic properties for lower concentration (0.5wt %) scaffolds.

Future Scope

1. Improved methods can be used to produce consistent porous structures on lower concentration scaffolds.
2. Use cyclical tests and predictions based on a cyclical stretch and hold basis with same hold time as that of stress-relaxation.
3. Similar methodology could be applied to other materials like synthetic polymers (PCL, PLGA) or other natural polymers (SIS, collagen), which may behave differently during stress-relaxation tests.
4. Use different combinations of pseudo-components to model stress-relaxation behavior of different materials based on their microstructure deformations during mechanical testing.
5. Compare the models in this study with other existing models like QLV by testing the model in study and its combinations at different loading rates.

This study is to put forward a sequential methodology to apply when analyzing the different viscoelastic characteristics of scaffolds and modeling their behavior.

REFERENCES

1. Abramowitch S. D, et al., *An evaluation of the quasi-linear viscoelastic properties of the healing medial collateral ligament in a goat model*. Ann Biomed Eng, 2004. **32**(3): p. 329-35.
2. Langer R and Vacanti JP, *Tissue Engineering*. Science, 1993. **260**(5110).
3. Jeffrey M. Karp, Paul D. Dalton, and M.S. Shoichet, *Scaffolds for Tissue Engineering*. MRS Bulletin, 2003.
4. Shoufeng Yang Ph.D., et al., *The Design of Scaffolds for Use in Tissue Engineering-Part I. Traditional Factors*. Tissue Engineering, 2001. **7**(6).
5. Dana L. Nettles M.S, Steven H. Elder Ph.D, and Jerome A. Gilbert Ph.D, *Potential Use of Chitosan as a Cell Scaffold Material for Cartilage Tissue Engineering*. Tissue Engineering, 2002. **8**(6).
6. Saito Naoto and T. Kunio, *New synthetic biodegradable polymers as BMP carriers for bone tissue engineering*. Biomaterials, 2003. **24**(13): p. 2287-2293.
7. Jeong Claire G and Hollister Scott J, *A comparison of the influence of material on in vitro cartilage tissue engineering with PCL, PGS, and POC 3D scaffold architecture seeded with chondrocytes*. Biomaterials, 2010. **31**(15): p. 4304-4312.
8. Malafaya Patrícia B, Silva Gabriela A, and R.R. L., *Natural-origin polymers as carriers and scaffolds for biomolecules and cell delivery in tissue engineering applications*. Advanced Drug Delivery Reviews, 2007. **59**(4-5): p. 207-233.
9. Pathiraja A.Gunatillake and R. Adhikari, *Biodegradable Synthetic Polymers for Tissue Engineering*. European Cells and Materials, 2003. **5**: p. 1-16.
10. Majeti N V and R. Kumar*, *A review of chitin and chitosan applications*. Reactive and Functional Polymers, 2000. **46**: p. 1-27.
11. Khor E and Lim Ly, *Implantable applications of chitin and chitosan*. Biomaterials, 2003. **24**(13): p. 2339-2349.
12. Dortmans L. J, Sauren A. A, and Rousseau E. P, *Parameter estimation using the quasi-linear viscoelastic model proposed by Fung*. J Biomech Eng, 1984. **106**(3): p. 198-203.
13. Aiba S-i, et al., *Covalent immobilization of chitosan derivatives onto polymeric film surfaces with the use of a photosensitive hetero-bifunctional crosslinking reagent*. Biomaterials, 1987. **8**: p. 481-488.
14. Hirano S, et al., *Formation of the Polyelectrolyte Complexes of Some Acidic Glycoasaminoglycans with partially N -Acetylated Chitosans*. Biopolymers, 1978. **17**: p. 805-810.
15. Kikuchi Y and Noda .A, *Polyelectrolyte Complexes of Heparin with Chitosan*. J Applied Polymer Science, 1976. **20**: p. 2561-2563.
16. Mao J S, et al., *Study of novel chitosan-gelatin artificial skin in vitro*. J Biomed Mater Res A, 2003. **64A**: p. 301-308.
17. Chung T, et al., *Preparation of alginate/galactosylated chitosan scaffold for hepatocyte attachment*. Biomaterials, 2002. **23**(14): p. 2827-34.
18. Li J, et al., *Culture of primary rat hepatocytes within porous chitosan scaffolds*. J Biomed Mater Res, 2003. **67A**(3): p. 938-43.

19. Shigemasa Y, et al., *Enzymatic degradation of chitins and partially deacetylated chitins*. Int J Biol Macromol, 1994. **16**(1): p. 43-49.
20. Huang Y, et al., *In vitro characterization of chitosan–gelatin scaffolds for tissue engineering*. Biomaterials, 2005. **26**(38): p. 7616-27.
21. Huang Y, Siewe M, and M. SV., *Effect of spatial architecture on cellular colonization*. Biotechnol Bioeng, 2006. **93**(1): p. 64-75.
22. Lawrence BJ, et al., *Multilayer composite scaffolds with mechanical properties similar to small intestinal submucosa*. J Biomed Mater Res A, 2008.
23. Moshfeghian A, Tillman J, and M. SV., *Characterization of emulsified chitosan–PLGA matrices formed using controlled-rate freezing and lyophilization technique*. J Biomed Mater Res A, 2006. **79**(2): p. 418-30.
24. He Jiankang a, et al., *Preparation of chitosan–gelatin hybrid scaffolds with well-organized microstructures for hepatic tissue engineering*. Acta Biomaterialia, 2009. **5**: p. 453-461.
25. Craiem D, *Fractional-order viscoelasticity applied to describe uniaxial stress relaxation of human arteries*. Phys Med Biol, 2008. **53**(17).
26. Defrate L.E and G. Li, *The prediction of stress-relaxation of ligaments and tendons using the quasi-linear viscoelastic model*. Biomech Model Mechanobiol, 2007. **6**(4).
27. Nekouzadeh, A., et al., *A simplified approach to quasi-linear viscoelastic modeling*. Journal of Biomechanics, 2007. **40**(14).
28. YC Fung, *Elasticity of soft tissues in simple elongation*. Am J Physiol, 1967. **213**(6): p. 1532-1544.
29. Nekouzadeh A and et al, *A simplified approach to quasi-linear viscoelastic modeling*. Journal of Biomechanics, 2007. **40**(14).
30. Craiem, D., et al., *Fractional-order viscoelasticity applied to describe uniaxial stress relaxation of human arteries*. Phys Med Biol, 2008. **53**(17).
31. Defrate L.E and G. Li, *The prediction of stress-relaxation of ligaments and tendons using the quasi-linear viscoelastic model*. Biomech Model Mechanobiol, 2007. **6**(4).
32. Rodriguez-Sanchez Kienzle, D.M., *Viscoelastic properties of chitosan*, in *Department of Nutrition and Food Science*. 1983, Massachusetts Institute of Technology. p. 161.
33. Mano, J.F., *Viscoelastic properties of chitosan with different hydration degrees as studied by dynamic mechanical analysis*. Macromol Biosci, 2008. **8**(1): p. 69-76.
34. Da Silva, J.A.L. and C.A.N.S. Santos, *Linear viscoelastic behavior of chitosan films as influenced by changes in the biopolymer structure*. Journal of Polymer Science Part B- Polymer Physics, 2007. **45**(14): p. 1907-1915.
35. Sakloetsakun, D., J.M. Hombach, and A. Bernkop-Schnurch, *In situ gelling properties of chitosan-thioglycolic acid conjugate in the presence of oxidizing agents*. Biomaterials, 2009. **30**(31): p. 6151-7.
36. Takahashi, M., et al., *Thermal and viscoelastic properties of xanthan gum/chitosan complexes in aqueous solutions*. Journal of Thermal Analysis and Calorimetry, 2006. **85**(3): p. 669-674.
37. Venault, A., et al., *Rheometric Study of Chitosan/Activated Carbon Composite Hydrogels for Medical Applications Using an Experimental Design*. Journal of Applied Polymer Science, 2011. **120**(2): p. 808-820.
38. Hsu, S.H., et al., *Evaluation of chitosan-alginate-hyaluronate complexes modified by an RGD-containing protein as tissue-engineering scaffolds for cartilage regeneration*. Artif Organs, 2004. **28**(8): p. 693-703.
39. Carlson B. M, *Principles of Regenerative Biology*. . Elsevier Inc., 2007.

40. Gabor M. H and H.R. D, *Parameters governing bacterial regeneration and genetic recombination after fusion of Bacillus subtilis protoplasts*. Journal of Bacteriology, 1979. **37**(3): p. 1346-1353.
41. Munro IR, G.B., "*Split-Rib Cranioplasty*". Annals of Plastic Surgery, 1981. **7**(5): p. 341-346.
42. Michalopoulos, G. and M. DeFrances, *Liver regeneration*. Science, 1997. **276**(5309): p. 60-66.
43. Michael and D.S. Rose, *Bio-Scalar Technology: Regeneration and Optimization of the Body-Mind Homeostasis*. 15th Annual AAAAM Conference: 2, 2007.
44. Higgins GM and R. Anderson, *Experimental pathology of the liver. I. Restoration of the liver of the white rat following partial surgical removal*. Arch. Pathol, 1931. **12**: p. 186-202.
45. Goldacre Ben, *The missing finger that never was*. 2008.
46. *Woman's persistence pays off in regenerated fingertip by Elizabeth Cohen*. CNN website, 2010.
47. *Liver Regeneration Unplugged*. Bio-Medicine, 2007.
48. *Regeneration recipe: Pinch of pig, cell of lizard*. Associated Press. MSNBC., 2007.
49. MacArthur BD and Oreffo RO *Bridging the Gap*. Nature, 2005. **433**(7021).
50. C.M. Agrawal and R.B. Ray, *Biodegradable polymeric scaffolds for musculoskeletal tissue engineering*. Journal of Biomedical Materials Research, 2001. **55**: p. 141-150.
51. Kumbar, S.G., *Electrospun nanofiber scaffolds: engineering soft tissues*. Biomedical Materials, 2008. **3**(3): p. 15.
52. Zhang, Y.Z., et al., *Characterization of the Surface Biocompatibility of the Electrospun PCL-Collagen Nanofibers Using Fibroblasts*. Biomacromolecules, 2005. **6**(5): p. 2583-2589.
53. Liu C, Xia Z, and C.J. T., *Design and Development of Three-Dimensional Scaffolds for Tissue Engineering*. Chemical Engineering Research and Design, 2007. **85**(7): p. 1051-1064.
54. A. Bacon, *Polymers – a synthetic or natural choice?* Drug Discovery Today, 2001. **7**(24): p. 1202-1203.
55. L. Lu, S.J. Peter, and M.D.L.e. al, *In vitro and in vivo degradation of porous poly(DL-lactic-co-glycolic acid) foams*. Biomaterials, 2000. **21**: p. 1837-1845.
56. G.P. Chen, T. Ushida, and T. Tateishi, *Development of biodegradable porous scaffolds for tissue engineering*. Materials Science and Engineering, 2001. **C 17**: p. 63-69.
57. Sio-Mei Lien, Wei-Te Li, and T.-J. Huang, *Genipin-crosslinked gelatin scaffolds for articular cartilage tissue engineering with a novel crosslinking method*. Materials Science and Engineering, 2008. **C 28**: p. 36-43.
58. Liu Xiaohua, et al., *Biomimetic nanofibrous gelatin/apatite composite scaffolds for bone tissue engineering*. Biomaterials, 2009. **30**(12): p. 2252-2258.
59. Li Mengyan, et al., *Electrospinning polyaniline-contained gelatin nanofibers for tissue engineering applications*. Biomaterials, 2006. **27**(13): p. 2705-2715.
60. Hu Min, et al., *Cell immobilization in gelatin-hydroxyphenylpropionic acid hydrogel fibers*. Biomaterials, 2009. **30**(21): p. 3523-3531.
61. Quynh P. Pham, * Upma Sharma Ph.D., and A.G.M. Ph.D., *Electrospinning of Polymeric Nanofibers for Tissue Engineering Applications: A Review*. Tissue Engineering, 2006. **125**.
62. Ma, L., et al., *Collagen/chitosan porous scaffolds with improved biostability for skin tissue engineering*. Biomaterials, 2003. **24**(26): p. 4833-4841.
63. Tan Huaping, et al., *Gelatin/chitosan/hyaluronan scaffold integrated with PLGA*

- microspheres for cartilage tissue engineering*. Acta Biomaterialia, 2009. **5**(1): p. 328-337.
64. Cooper Ashleigh, Bhattarai Narayan, and Z. Miqin, *Fabrication and cellular compatibility of aligned chitosan-PCL fibers for nerve tissue regeneration*. Carbohydrate Polymers, 2011. **85**(1): p. 149-156.
 65. Ma Lie, et al., *Collagen/chitosan porous scaffolds with improved biostability for skin tissue engineering*. Biomaterials, 2003. **24**(26): p. 4833-4841.
 66. Thorvaldsson, A., et al., *Controlling the architecture of nanofiber-coated microfibers using electrospinning*, Wiley Subscription Services, Inc., A Wiley Company. p. 511-517.
 67. Inai, R., M. Kotaki, and S. Ramakrishna, *Deformation behavior of electrospun poly(L-lactide-co-ε-caprolactone) nonwoven membranes under uniaxial tensile loading*. 2005, Wiley Subscription Services, Inc., A Wiley Company. p. 3205-3212.
 68. Feng, C., K.C. Khulbe, and T. Matsuura, *Recent progress in the preparation, characterization, and applications of nanofibers and nanofiber membranes via electrospinning/interfacial polymerization*, Wiley Subscription Services, Inc., A Wiley Company. p. 756-776.
 69. E. Sachlos and J.T. Czernuszka*, *Making Tissue Engineering Scaffolds work-Review on the Application of Solid Freeform Fabrication Technology to the Production of Tissue Engineering Scaffolds*. European Cells and Materials, 2003. **5**: p. 29-40.
 70. Nicolle S and P.J. F, *Dehydration effect on the mechanical behaviour of biological soft tissues: Observations on kidney tissues*. Journal of the Mechanical Behavior of Biomedical Materials, 2010. **3**(8): p. 630-635.
 71. Hollister S. J, Maddox R. D, and T.J. M., *Optimal design and fabrication of scaffolds to mimic tissue properties and satisfy biological constraints*. Biomaterials, 2002. **23**(20): p. 4095-4103.
 72. Hollister S.J, *Scaffold Design and Manufacturing: From Concept to Clinic*. Advanced Materials, 2009. **21**(32-33): p. 3330-3342.
 73. Arltan Serdar, Oyadiji S. Olutunde, and B.R. M., *A mechanical model representation of the in vivo creep behaviour of muscular bulk tissue*. Journal of Biomechanics, 2008. **41**(12): p. 2760-2765.
 74. Roderic Lakes, *Viscoelastic Materials*. 2009.
 75. Meyers and Chawla, *"Mechanical Behavior of Materials*. 1999: p. 98-103.
 76. Y.C. Fung, N. Perrone, and M. Anliker, *Biomechanics- Its foundations and objectives*. 1972.
 77. Guillemenet J, Bistac S, and S. J, *Relationship between polymer viscoelastic properties and adhesive behaviour*. International Journal of Adhesion and Adhesives, 2002. **22**(1): p. 1-5.
 78. McCrum, Buckley, and Bucknell, *Principles of Polymer Engineering*. 2003.
 79. Van Loocke M, Simms C. K, and L.C. G, *Viscoelastic properties of passive skeletal muscle in compression--Cyclic behaviour*. Journal of Biomechanics, 2009. **42**(8): p. 1038-1048.
 80. Ciarletta P, et al., *A novel microstructural approach in tendon viscoelastic modelling at the fibrillar level*. Journal of Biomechanics, 2006. **39**(11): p. 2034-2042.
 81. Huyghe Jacques M, et al., *The constitutive behaviour of passive heart muscle tissue: A quasi-linear viscoelastic formulation*. Journal of Biomechanics, 1991. **24**(9): p. 841-849.
 82. Dehoff P. H, *On the nonlinear viscoelastic behavior of soft biological tissues*. Journal of Biomechanics, 1978. **11**(1-2): p. 35-40.
 83. Cohen R. E, Hooley C. J, and M.N. G, *Viscoelastic creep of collagenous tissue*. Journal of Biomechanics, 1976. **9**(4): p. 175-184.
 84. Humphrey J D, *Review: Paper: Continuum Biomechanics of soft biological tissues*. The

- Royal Society, 2003. **459**: p. 3-46.
85. Robert Lanza, Rober Langer, and J. Vacanti, *Principles of Tissue Engineering*. 2007.
 86. *Stress-relaxation test*. Encyclopedia Britannica Online, 2011.
 87. Madihally, S.V., *Principles of Biomedical engineering*. 2010.
 88. Joseph J. Sarver, Paul S. Robinson, and Dawn M. Elliott*, *Methods for Quasi-Linear Viscoelastic Modeling of Soft Tissue: Application to Incremental Stress-Relaxation Experiments*. ASME, 2003. **125**: p. 754-758.
 89. Mirani, R.D., et al., *The stress relaxation characteristics of composite matrices etched to produce nanoscale surface features*. Biomaterials, 2009. **30**(5): p. 703-10.
 90. Iyer, M.S. and R.R. Rhinehart, *A method to determine the required number of neural-network training repetitions*. IEEE Trans Neural Netw, 1999. **10**(2): p. 427-32.
 91. Jiankang He, et al., *Fabrication and characterization of chitosan/gelatin porous scaffolds with predefined internal microstructures*. Polymer, 2007. **48**(15): p. 4578-4588.
 92. Zheng Jun Ping, et al., *Preparation of biomimetic three-dimensional gelatin/montmorillonite-chitosan scaffold for tissue engineering*. Reactive and Functional Polymers, 2007. **67**(9): p. 780-788.
 93. Duling R. R, et al., *Mechanical characterization of electrospun polycaprolactone (PCL): a potential scaffold for tissue engineering*. J Biomech Eng, 2008. **130**(1): p. 011006.
 94. Silver F. H, Freeman J. W, and D. D, *Viscoelastic properties of human skin and processed dermis*. Skin Res Technol, 2001. **7**(1): p. 18-23.
 95. Bouhout Sara, et al., *Bladder substitute reconstructed in a physiological pressure environment*. Journal of Pediatric Urology. **In Press, Corrected Proof**.
 96. Sarasam A and M.S. V, *Characterization of chitosan-polycaprolactone blends for tissue engineering applications*. Biomaterials, 2005. **26**(27): p. 5500-8.
 97. J. D. Humphrey, *Review: Paper: Continuum Biomechanics of soft biological tissues*. The Royal Society, 2003. **459**: p. 3-46.
 98. Joseph J. Sarver, Paul S. Robinson, and D.M. Elliott, *Methods for Quasi-Linear Viscoelastic Modeling of Soft Tissue: Application to Incremental Stress-Relaxation Experiments*. ASME, 2003. **125**: p. 754-758.
 99. Li L P and Herzog W, *The role of viscoelasticity of collagen fibers in articular cartilage: theory and numerical formulation*. Biorheology, 2004. **41**(3-4): p. 181-94.
 100. Taylor Z. A, et al., *On modelling of anisotropic viscoelasticity for soft tissue simulation: numerical solution and GPU execution*. Med Image Anal, 2009. **13**(2): p. 234-44.
 101. Roderic Lakes, *Viscoelastic Materials*. 2009, Cambridge University Press -Technology and Engineering.
 102. Delphine S. Perie, et al., *Correlating Material Properties with Tissue Composition in Enzymatically Digested Bovine Annulus Fibrosus and Nucleus Pulposus Tissue*. Annals of Biomedical Engineering, 2006. **34**(5): p. 769-777.
 103. L.P. Li, et al., *The Role of Viscoelasticity of Collagen Fibers in Articular Cartilage: Axial Tension Versus Compression*. Medical Engineering & Physics, 2005. **27**(1): p. 51-57.
 104. Kornkarn Makornakaewkeyoon, *Polycaprolactone Matrices generated in aqueous media: Natural Polymers Immobilization and Stress-Relaxation behavior.*, in *Chemical Engineering 2010*, Oklahoma State University: Stillwater. p. 74.
 105. Upasana M. Sridhar, *Converting Ramp-Hold Test Data to Cyclical Tests Using Pseudo-Component Viscoelastic Models*, in *Chemical Engineering*. 2010, Oklahoma State University: Stillwater.
 106. Rhinehart R. R, M Su, and Upasana. M. Sridhar, *Leapfrogging: a novel optimization approach*, in *European Journal of Optimizations Research*. 2009.

APPENDICES

APPENDIX 1

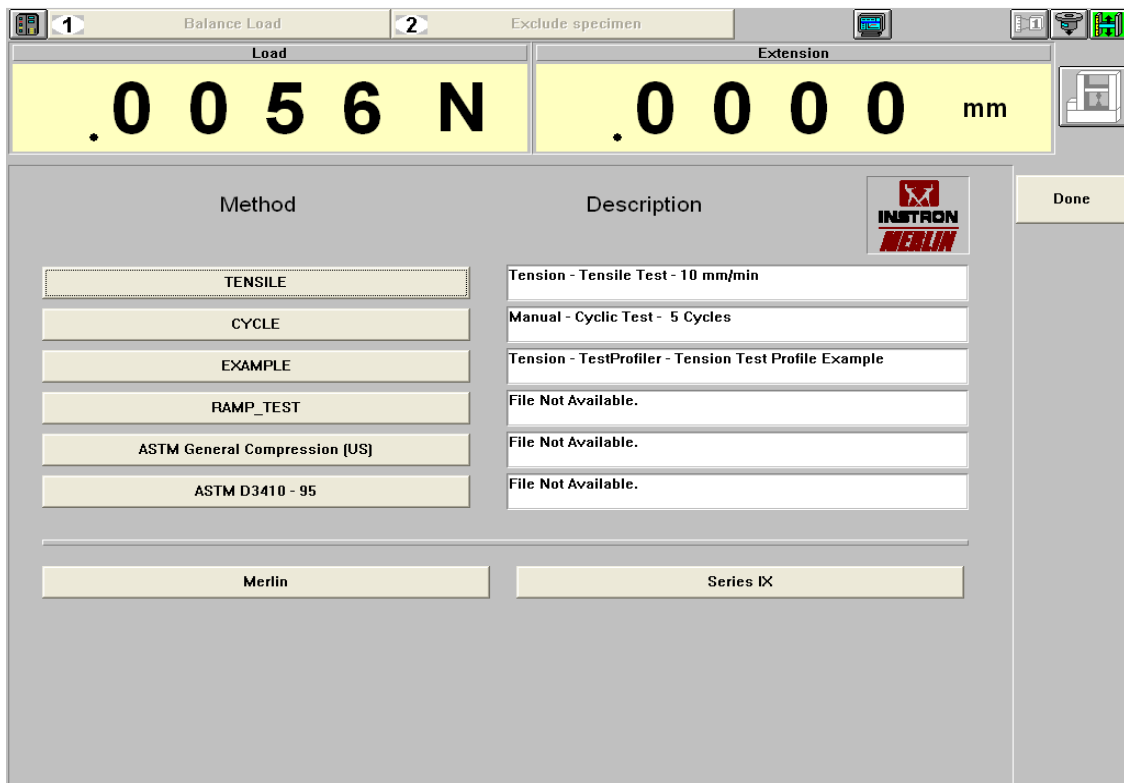
TENSILE TEST SET UP

Step 1:

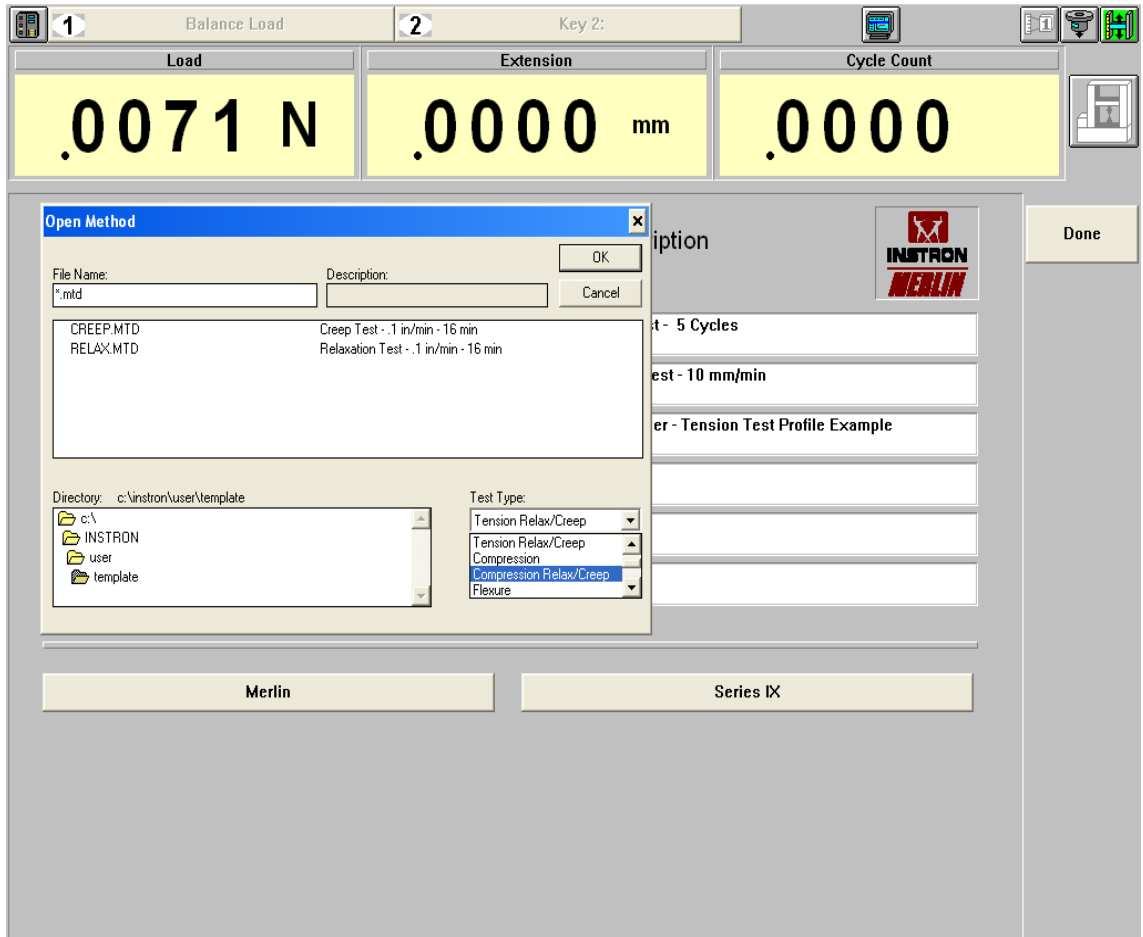
First start the INSTRON 5542 machine using an on/off switch at the back.

Open the MERLIN software by double clicking its icon on the computer desktop.

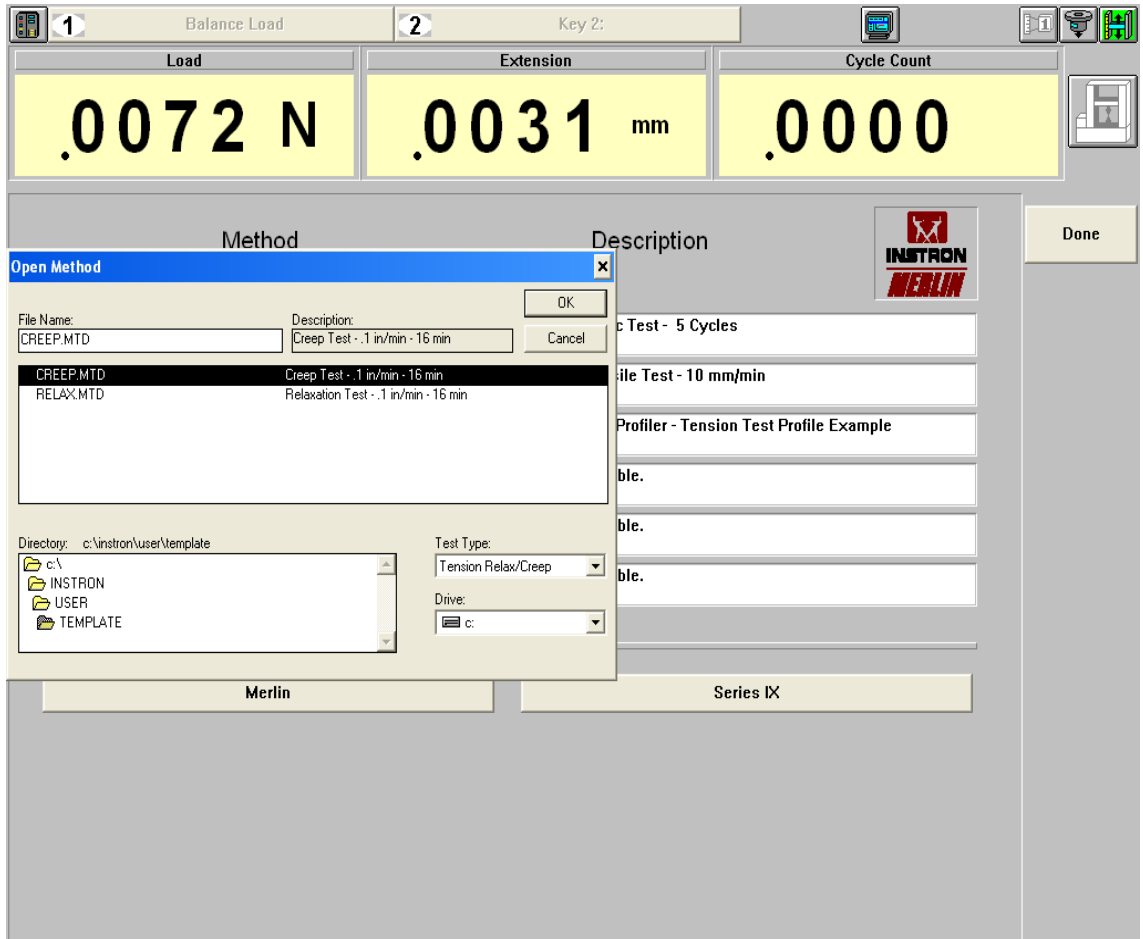
The window shown below appears on the screen, called the QuickOpen screen.



Usually the test types are mentioned as above. If the test type you want is not seen, then click the Merlin tab. An open method screen appears as shown below.




You can select the test type you want and that appears as a tab on QuickOpen screen.



Once it is selected the main menu opens where you can see the test added as shown below.

1 Balance Load 2 Key 2:

| Load | Extension | Time |
|-----------|-----------|-----------|
| .0017 lbf | .0000 in | .0000 min |



| Method | Description |
|-------------------------------|---|
| CREEP | TensionRC - Creep Test - .1 in/min - 16 min |
| CYCLE | Manual - Cyclic Test - 5 Cycles |
| TENSILE | Tension - Tensile Test - 10 mm/min |
| EXAMPLE | Tension - TestProfiler - Tension Test Profile Example |
| RAMP_TEST | File Not Available. |
| ASTM General Compression (US) | File Not Available. |

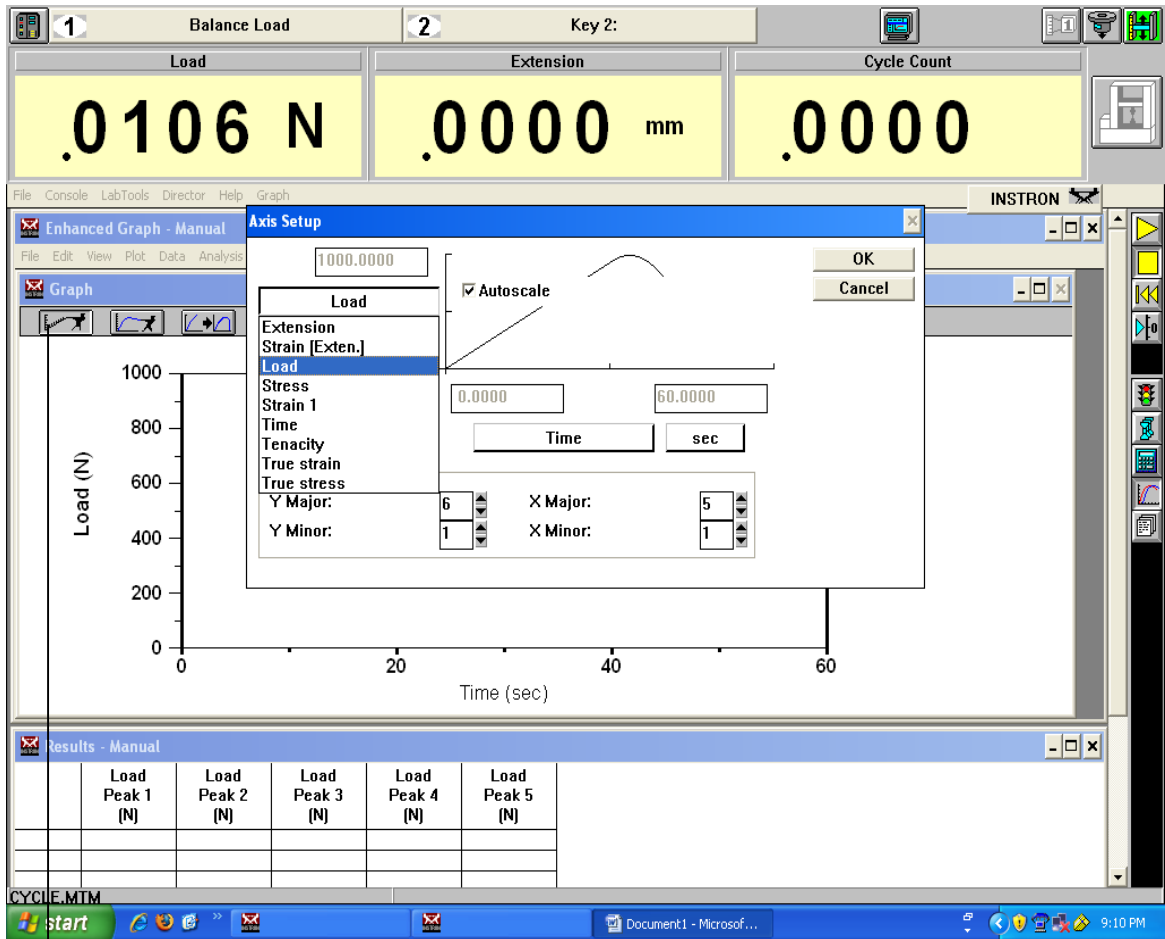
| | |
|--------|-----------|
| Merlin | Series IX |
|--------|-----------|

You can also change what you want to see and their units on the screen as shown below.

The screenshot displays the INSTRON software interface. At the top, there are three digital readouts (DROs) for 'Extension' (0.0000 in) and 'Time' (0.0000 min). Below these are several data selection menus. The 'Tensile strain' menu is set to 'mil', and the 'Extension' menu is selected. A graph titled 'Creep Relaxation' is visible, showing a plot of strain versus time. At the bottom, there is a 'Results - Tension Relax/Creep' table with the following structure:

| | Max Load (lbf) | Strain at 0.5 min (%) | Strain at 1 min (%) | Strain at 2 min (%) | Strain at 4 min (%) | Strain at 8 min (%) | Strain at 16 min (%) | Total Creep (%) |
|--|----------------|-----------------------|---------------------|---------------------|---------------------|---------------------|----------------------|-----------------|
| | | | | | | | | |
| | | | | | | | | |
| | | | | | | | | |

You can change the X and Y axes by clicking on the tabs on the graph toolbar as shown.



Graph

Click the Test control Lab Tool and in the Motion button, set the rate at which you want the sample to be pulled.

The screenshot displays the INSTRON software interface. At the top, there are three main data fields: **Load** showing **.0109 N**, **Extension** showing **.0000 mm**, and **Cycle Count** showing **.0000**. Below these is a menu bar with options: File, Console, LabTools, Director, Help. The main window contains several panels:

- Enhanced Graph - Manual**: A graph window with a toolbar and a menu bar (File, Edit, View, Plot, Data, Analysis, Tools, Format, Window, Help). The graph area is currently blank.
- Test Control - Manual**: A control panel with a sidebar (Motion, Events, Cycling, Data) and a main area with the following settings:
 - Ramp**: Ctrl. mode: Extension, Speed: 1.0000 mm/sec
 - Direction at start**: Radio buttons for Up (selected) and Down
 - Break**: Enabled, Sensitivity: 4.0e+1%, Action: Stop
- Sample - Manual**: A specimen definition window with a sidebar (Define, Specimen, Notes, User Inputs) and a main area:
 - Number: 1 (Untested), Excluded, Reject Enable
 - Buttons: Measure..., Next, Reject
 - Specimen name: Chitosan
 - Comment: 1
 - Dimensions table:

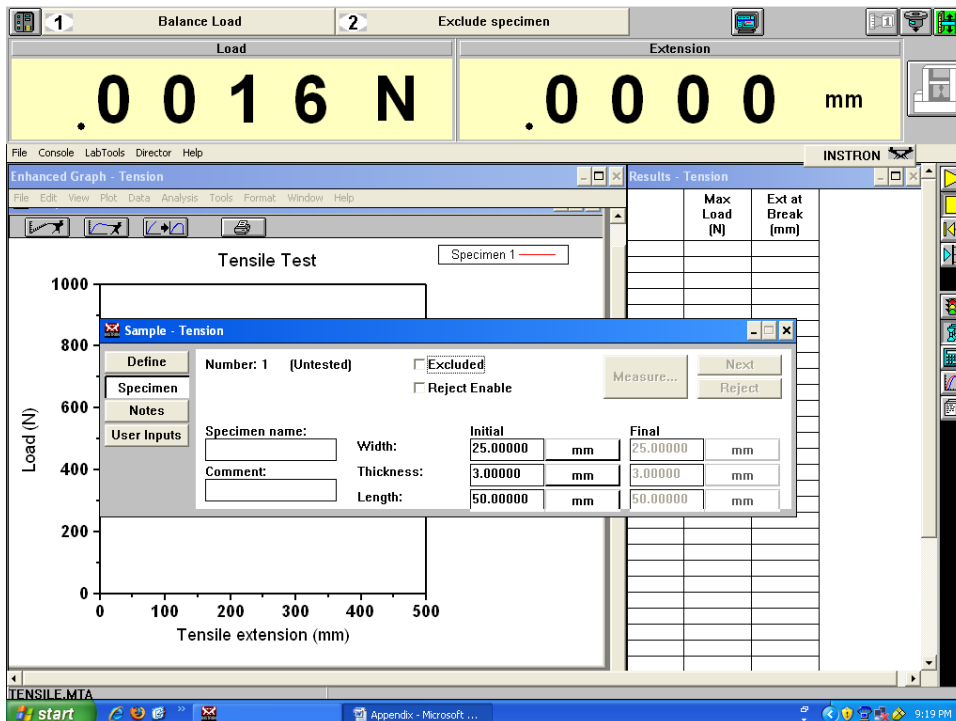
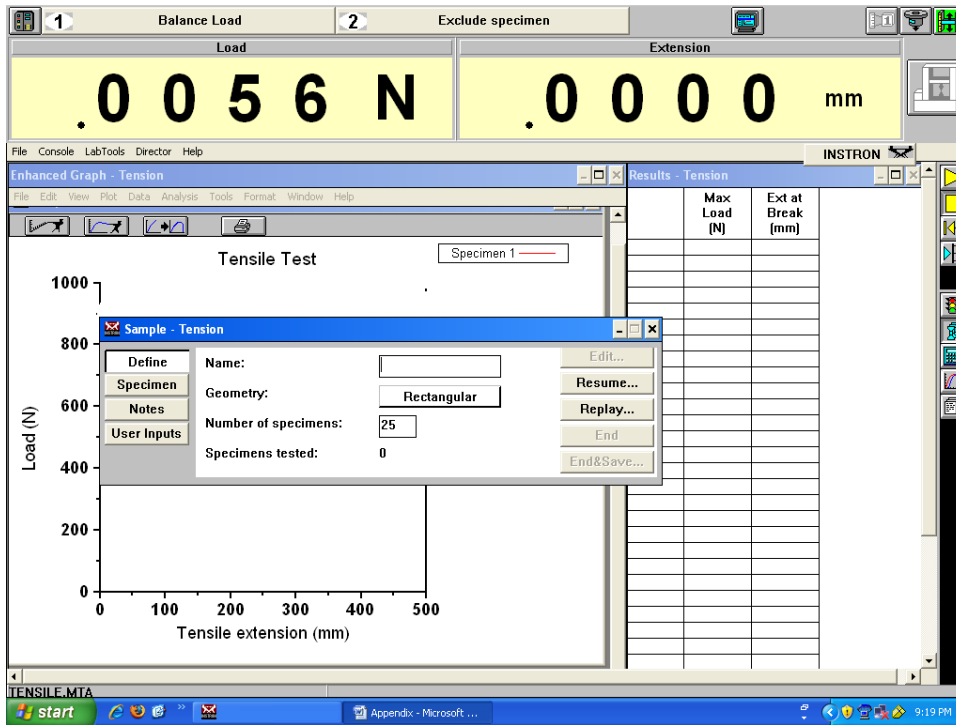
| | Initial | Final |
|------------|-------------|-------------|
| Width: | 10.00000 mm | 10.00000 mm |
| Thickness: | 4.00000 mm | 4.00000 mm |
| Length: | 40.00000 mm | 40.00000 mm |

The Windows taskbar at the bottom shows the start button, several icons, and the system tray with the time 9:13 PM.

Step 3:

Give information about the sample by clicking the Sample Lab Tool.

You can define the sample using Define button and give its dimensions in the Specimen button as shown below.

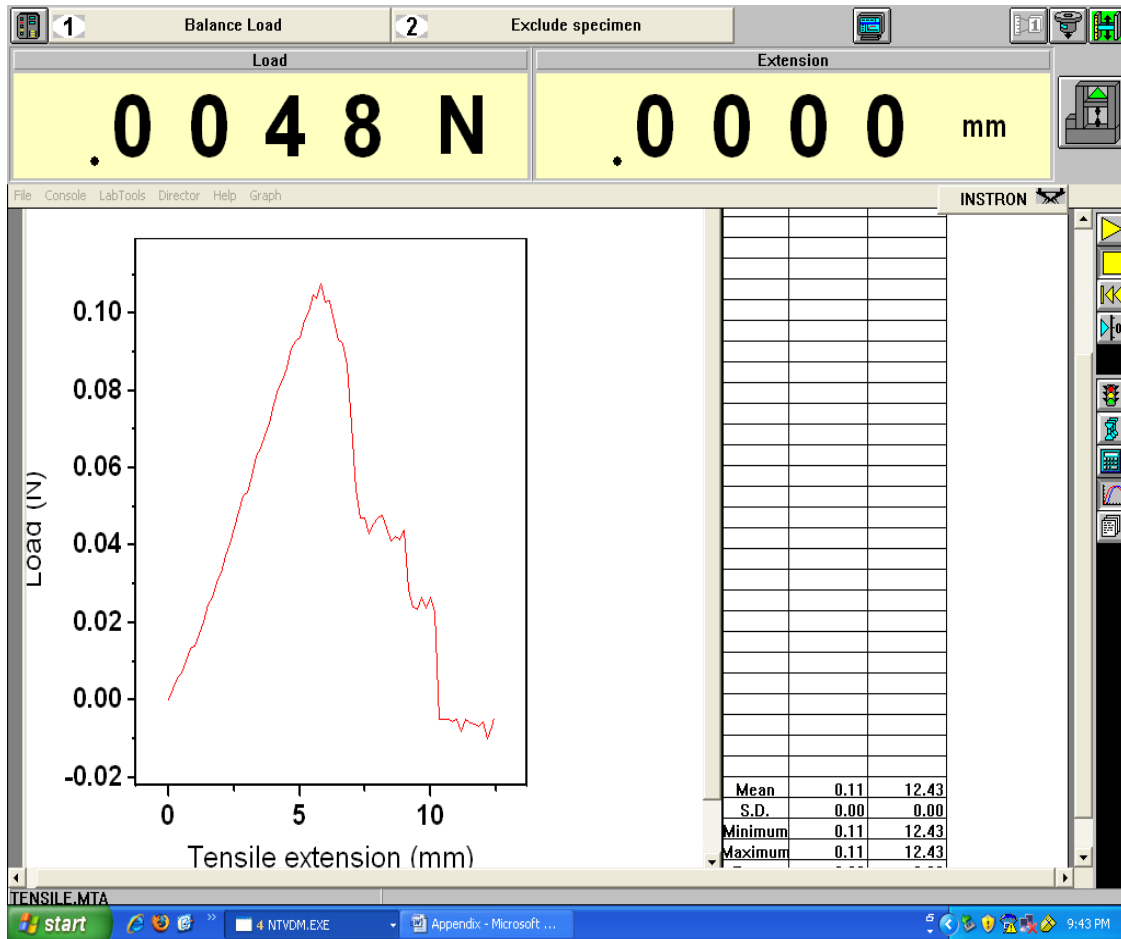


Step 4:

Fix the sample in the grips provided and reset gauge length and load to zero using the “RESET GL” on the control panel and Balance load button on main screen, respectively.

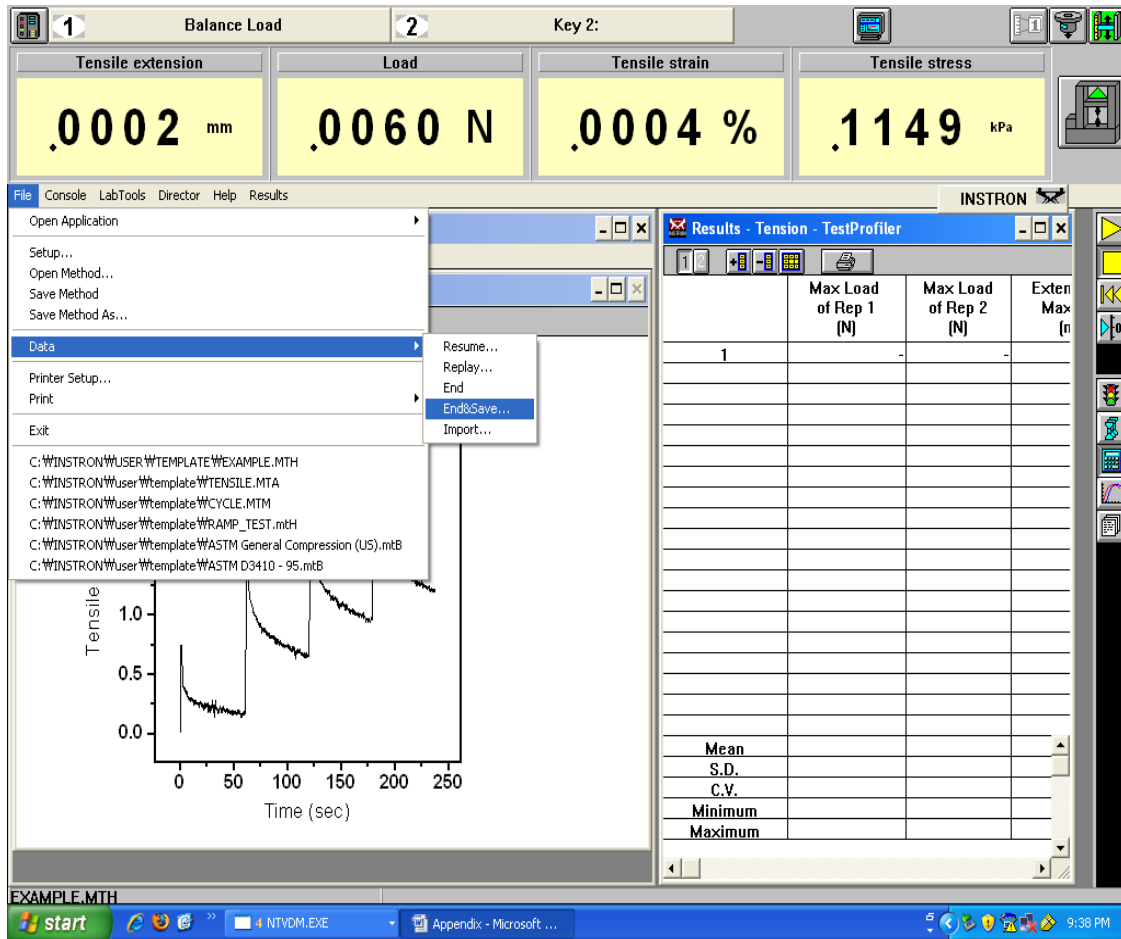
Click the yellow start button for the test to start.

A Strain vs. Stress curve is attained as shown in figure.



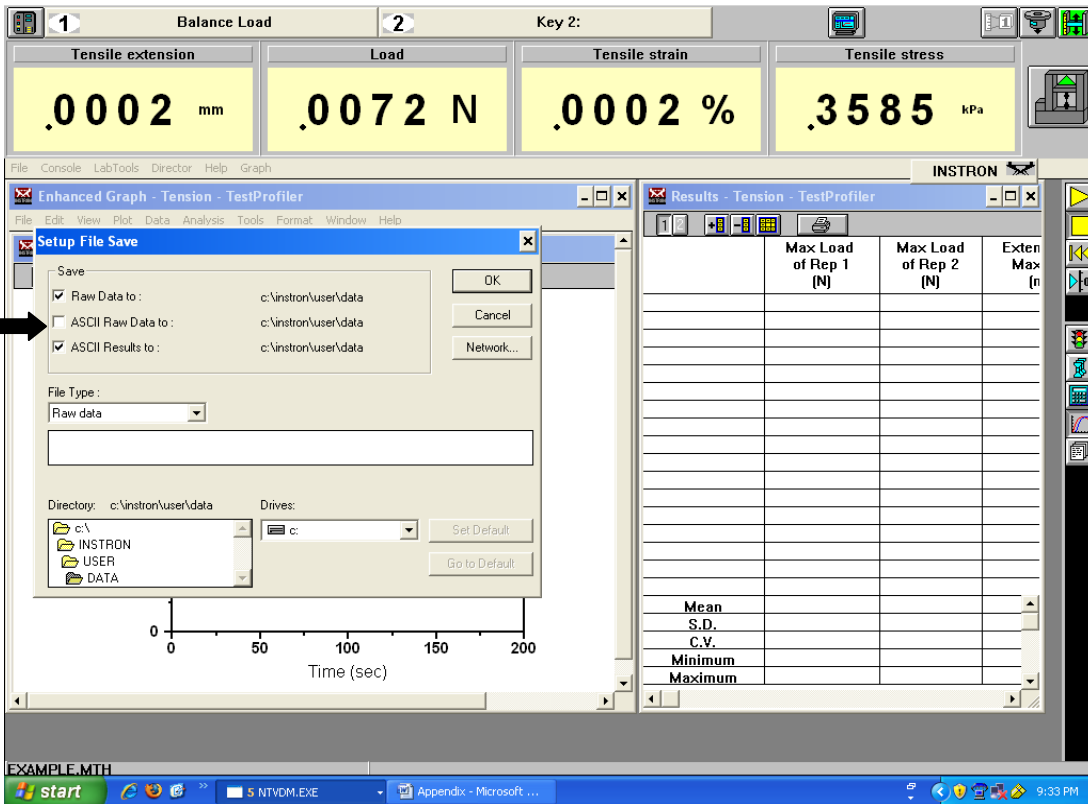
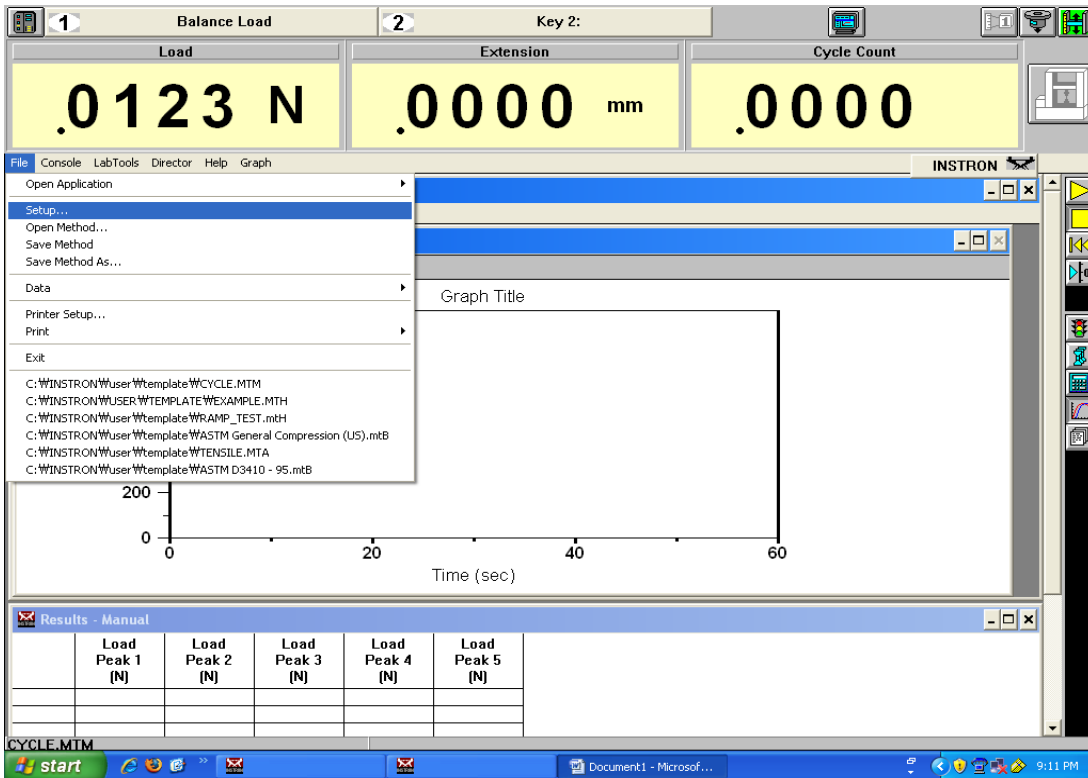
Step 5

To Save data → Upper File menu → Data → End and Save Data → give a file name.



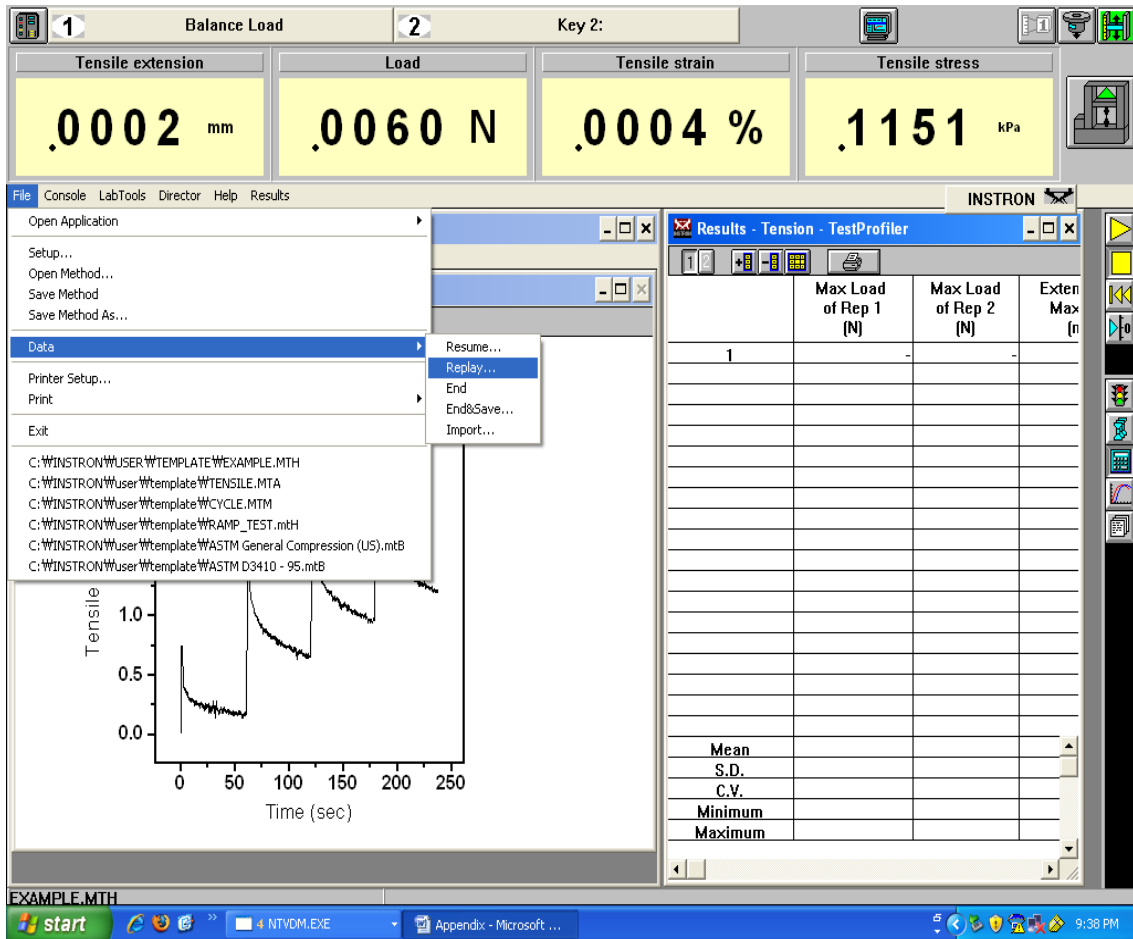
You have to make sure the data is saved as a raw file (<filename>.raw).

To check that go to Upper file menu → Setup → check on ASCII as shown below.



Step 6

If you forgot to save the data with the raw extension then go to File menu → Data → Replay as shown below.

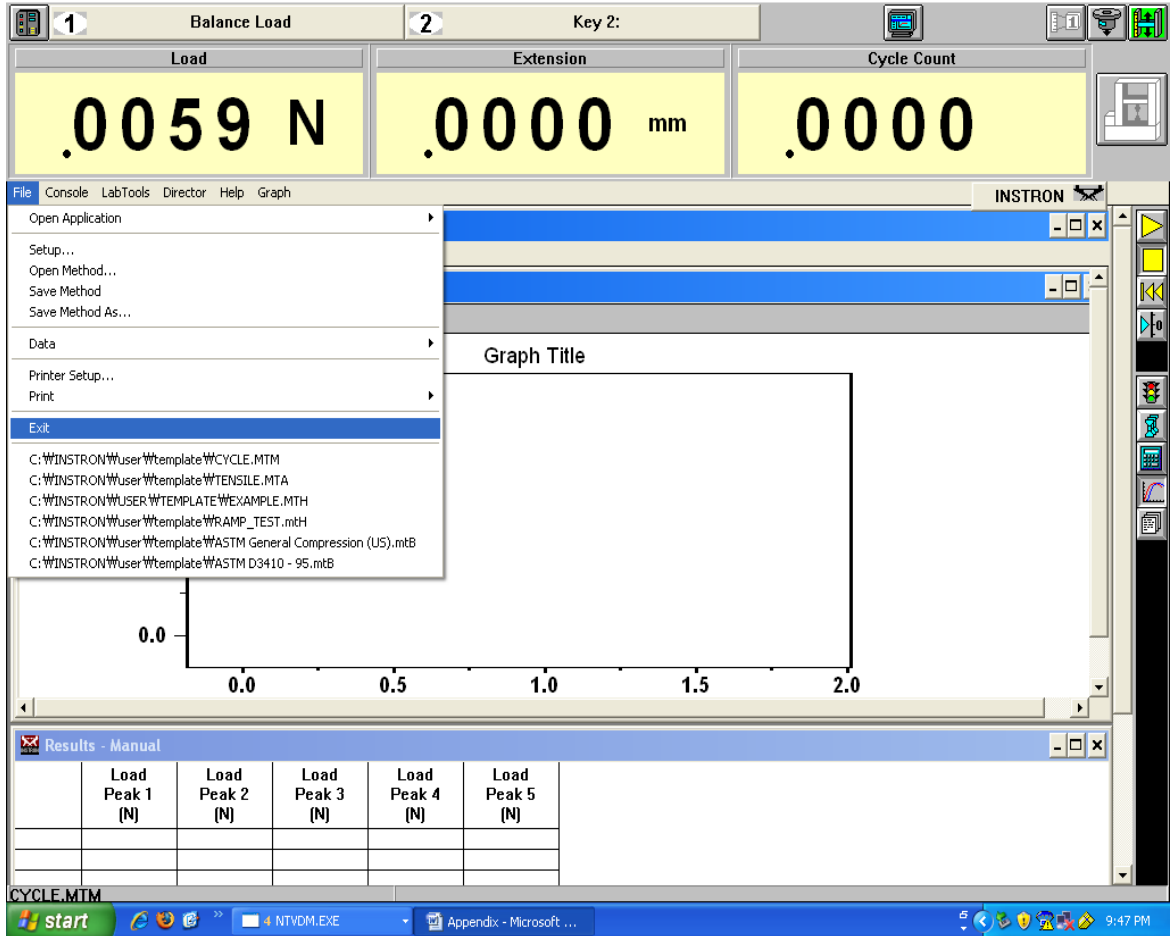


Then the result shows up depending on the test type (tensile-ramp-cyclic)-then make changes in specifications n go ahead n save like the usual-go ahead and then save

You can make changes in specifications-the type of graph you want to look at also.

Step 7

After the data has been saved, you can exit from the test as shown below.



STRESS-RELAXATION TEST

Step 1

Choose the ramp and hold method from the main menu.



If the ramp_hold tab doesn't exist on the quickscreen menu then click on the Example tab as shown above.

Step 2

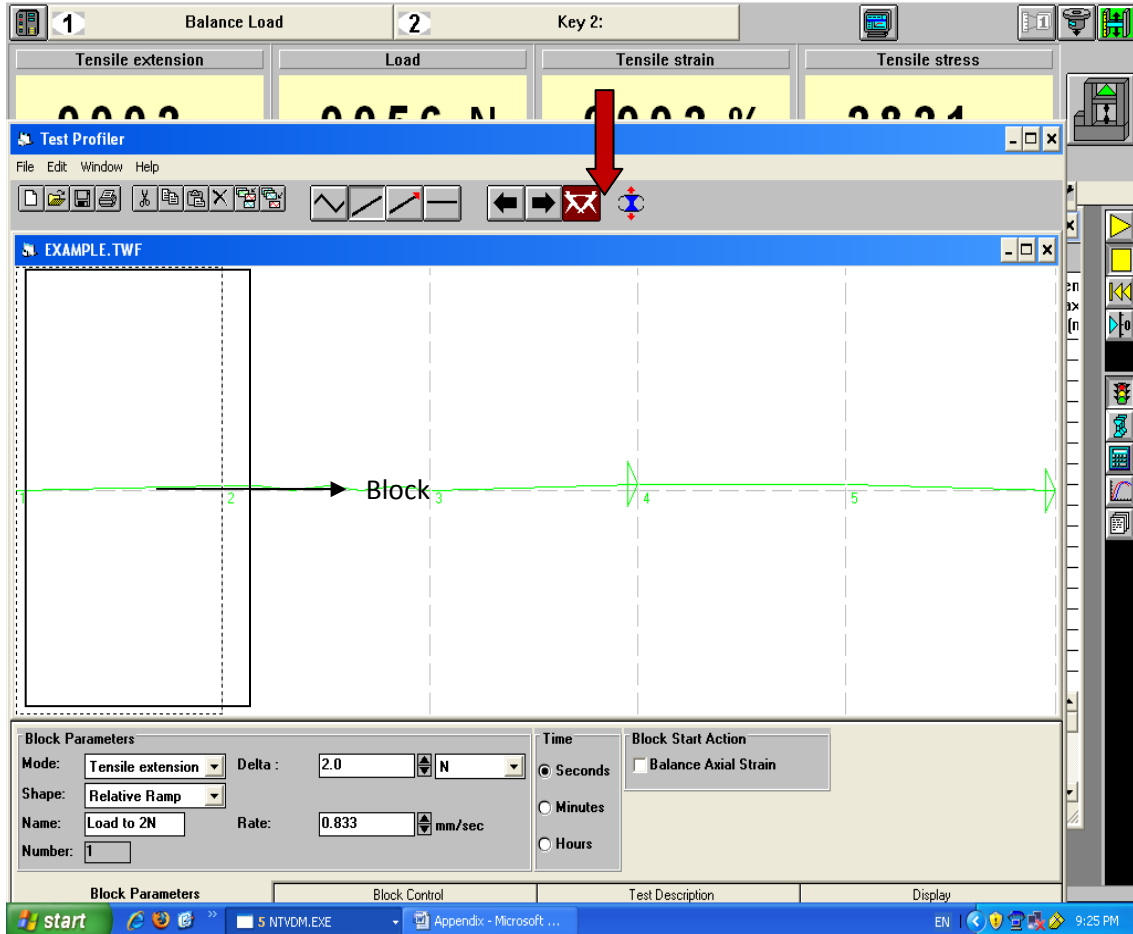
A screen as shown below appears. Here you can click on the Test Control Lab Tool → Test Tab → Profiler to specify the parameters for the stress relaxation test.

The screenshot displays the INSTRON Test Control software interface. At the top, four large yellow boxes show real-time data: Tensile extension (.0002 mm), Load (.0046 N), Tensile strain (.0002 %), and Tensile stress (.2278 kPa). Below this is a menu bar with 'File', 'Console', 'LabTools', 'Director', and 'Help'. The main window contains several panes: 'Enhanced Graph - Tension - TestProfiler', 'Results - Tension - TestProfiler', and 'Test Control - Tension - TestProfiler'. The 'Test Control' window is the active foreground window, showing a 'Main test profile' section with a 'Profile' dropdown set to 'EXAMPLE' and buttons for 'Browse...' and 'Profiler...'. Below this is a 'Description' field containing the text: 'Load to 2N then balance Axial Strain and cycle 3 times. Absolute Ramp to 15mm and Hold for 10sec Return and then repeat from Block 2.' The 'Test stop' section includes 'Criteria' (Load) with a 'Value' of 500.000 N and 'Action' (Return) with a 'Delay' of 5.00 sec. A graph at the bottom left shows a plot of 'Time (sec)' from 0 to 200. To the right of the graph is a table with columns for 'Max Load of Rep 1 (N)', 'Max Load of Rep 2 (N)', and 'Exten Max (n)'. The table has several rows, with the last row containing 'Mean', 'S.D.', 'C.V.', 'Minimum', and 'Maximum'. The Windows taskbar at the bottom shows the 'start' button, several open applications including 'Test Director', and the system clock showing '9:24 PM'.

Step 3

After you click on profiler a window as shown below appears.

Here we can assign the number of ramp and hold stages we want by adding blocks.



To add blocks click on the arrow button as pointed out in the above picture.

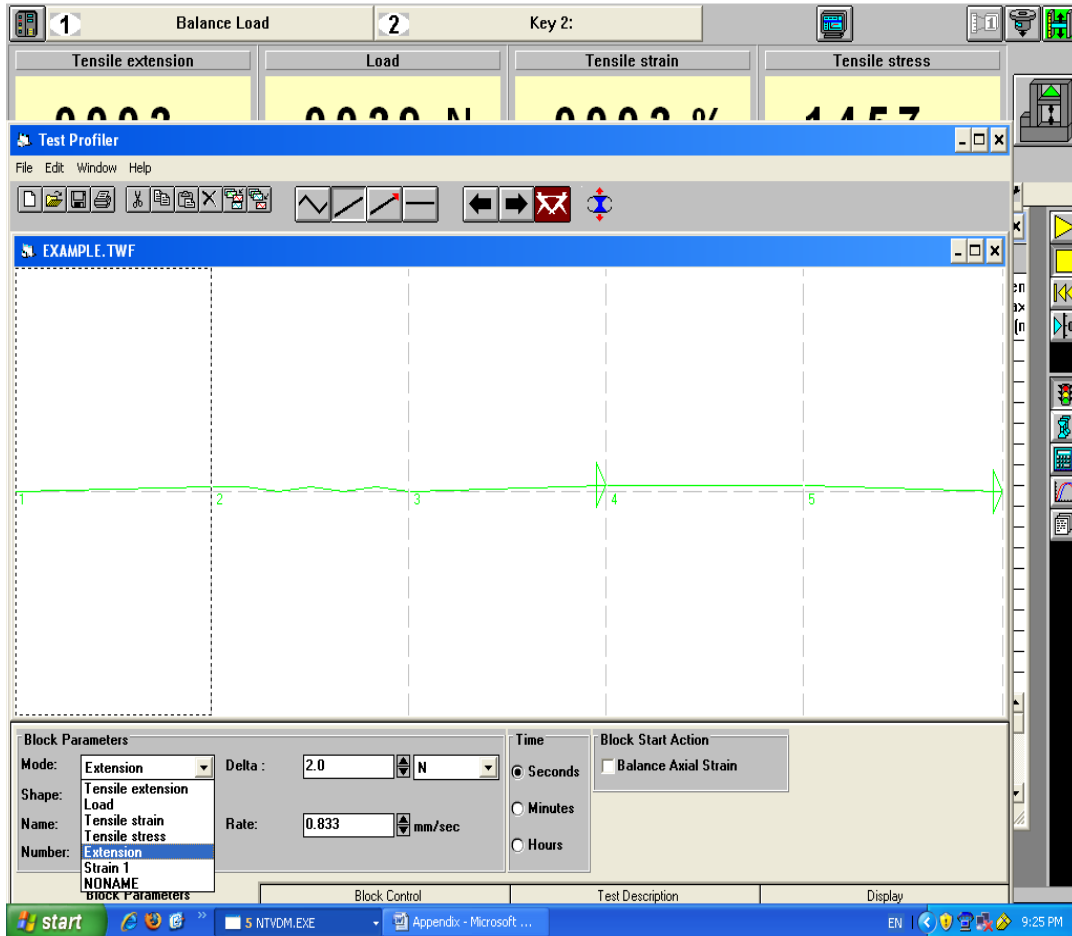
For my experiment I used 10 blocks. 5 for ramp and 5 for hold together they make 5 ramp and hold stages.

Step 4

Once the blocks are added, we need to give specifications for each block by clicking on the block.

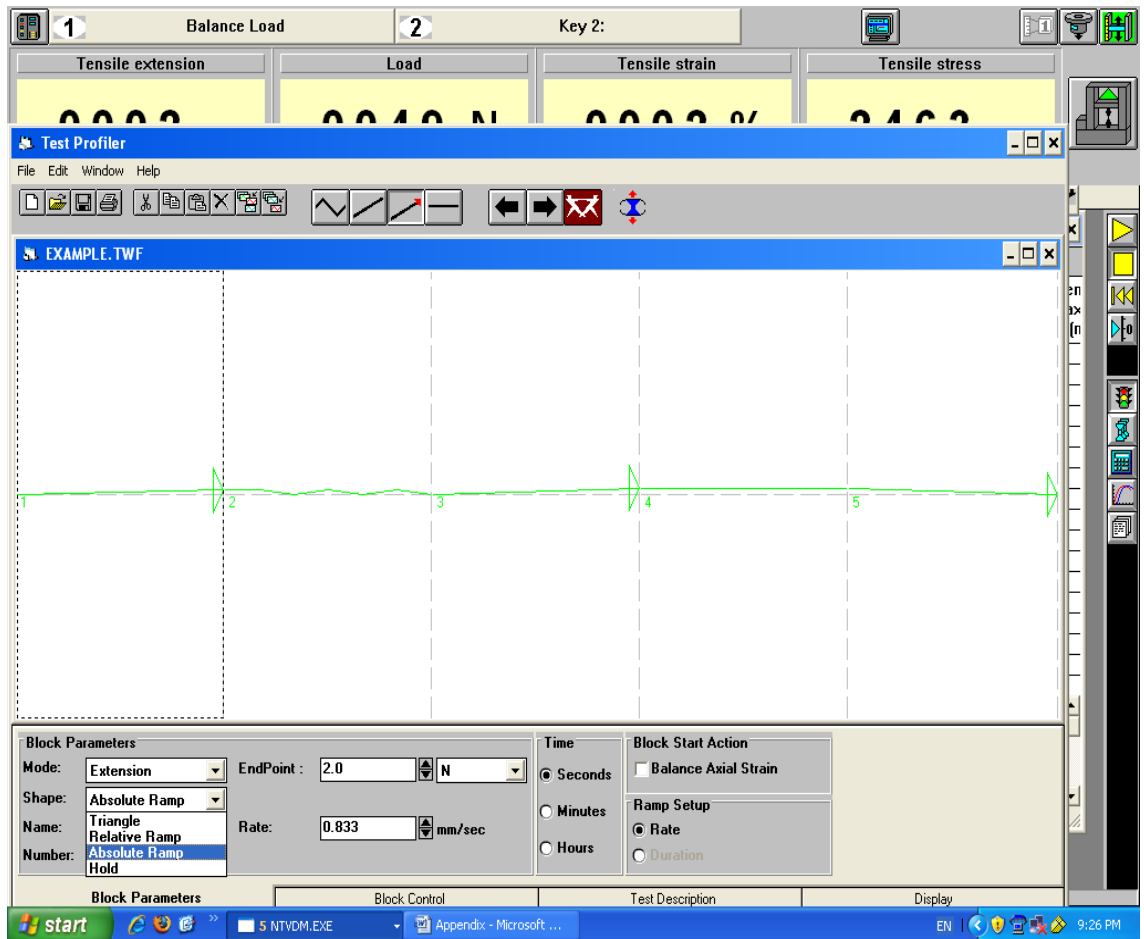
The first block will be the ramp and the second will be hold. So every odd block will have specifications for ramp and every even block will have specifications for hold.

Now, click on the first block as shown below. And in the block parameters section enter the specifications.



For the first block which is the ramp phase, In the mode field select Extension.

And for the shape field select Absolute ramp from the drop down menu as shown below.



You can specify the endpoint of the ramp phase in the “EndPoint” field and also the units. “In this case it was strain (5%). You can also specify the rate (2.5mm/s) at which the sample is pulled in the rate field.

Repeat step 4 for every odd block which defines the ramp phase. And for the endpoint for every ramp phase has to be higher than the previous stage and in constant increments. For example if you fix the strain limit to 5% then first block’s end point will be 5%, 10% for third block, 15% for the 5th block,etc. But the rate of pulling is constant.

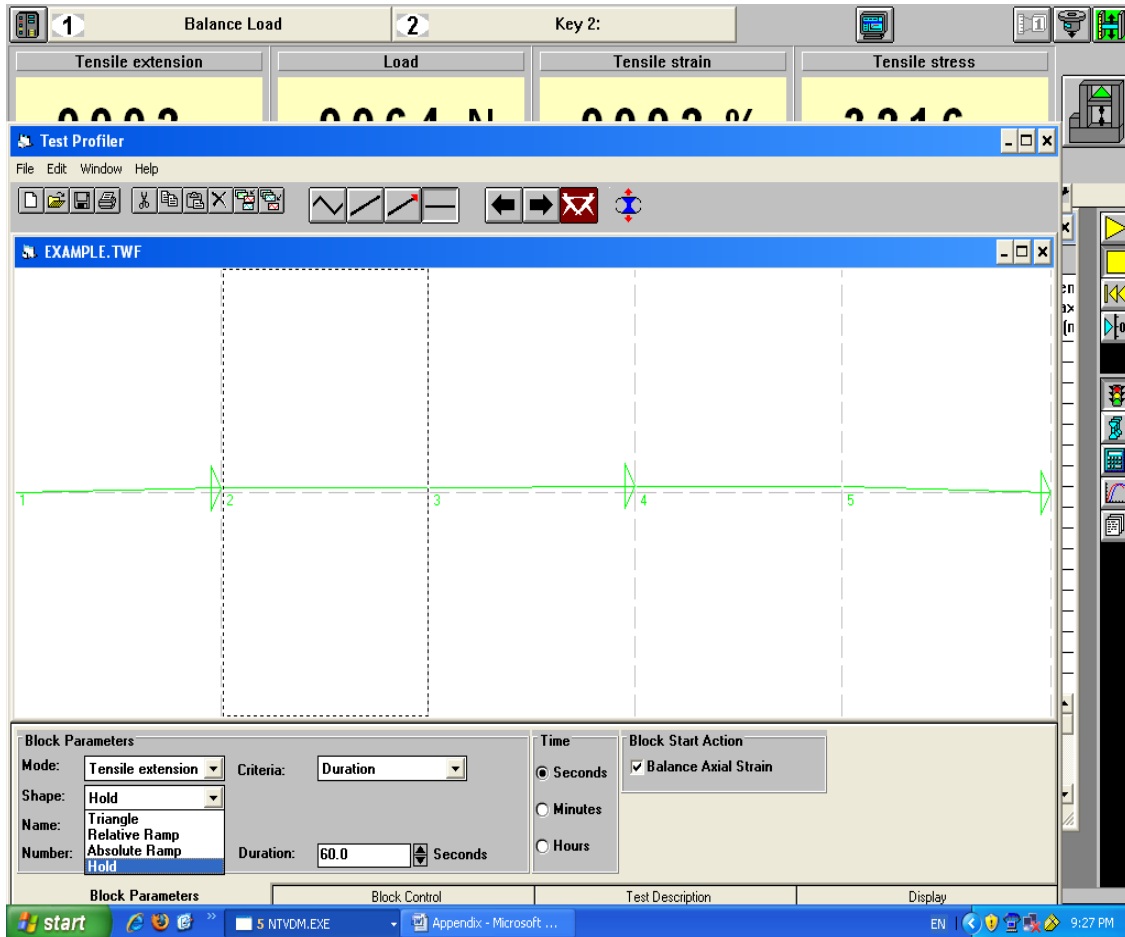
Step 5

For hold block select Tensile extension for the Mode field and Hold for the shape field as shown below.

The screenshot displays the Test Profiler software interface. At the top, there are tabs for 'Balance Load' and 'Key 2:'. Below these are four data fields: 'Tensile extension' (0000), 'Load' (0050 N), 'Tensile strain' (0000 %), and 'Tensile stress' (0001). The main window is titled 'Test Profiler' and contains a menu bar (File, Edit, Window, Help) and a toolbar with various icons. Below the toolbar is a graph area showing a green waveform with five marked points (1, 2, 3, 4, 5) and vertical dashed lines. The bottom section contains 'Block Parameters' with the following settings:

| Block Parameters | | Time | Block Start Action |
|-------------------------|--------------------|--|--|
| Mode: Tensile extension | Maximum: 10.0 mm | <input checked="" type="radio"/> Seconds | <input checked="" type="checkbox"/> Balance Axial Strain |
| Shape: Triangle | Minimum: 0.0 mm | <input type="radio"/> Minutes | Initial Waveform Direction |
| Name: Triangle | Rate: 8.333 mm/sec | <input type="radio"/> Hours | <input checked="" type="radio"/> Maximum Limit |
| Number: 2 | Cycles: 3.0 | | <input type="radio"/> Minimum Limit |

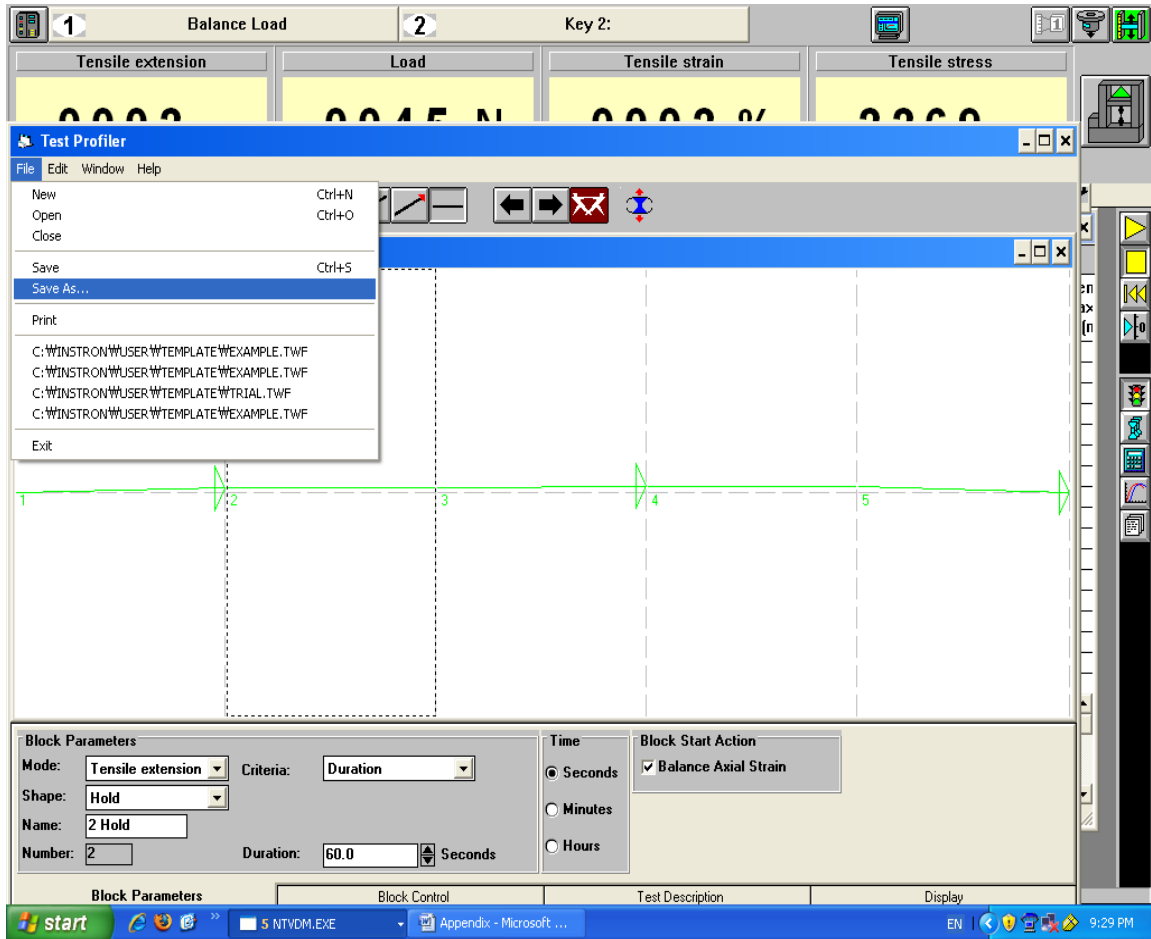
The Windows taskbar at the bottom shows the start button, several open applications, and the system tray with the time 9:26 PM.



Set the criteria to be duration and give the duration. In my case it was 58 seconds.

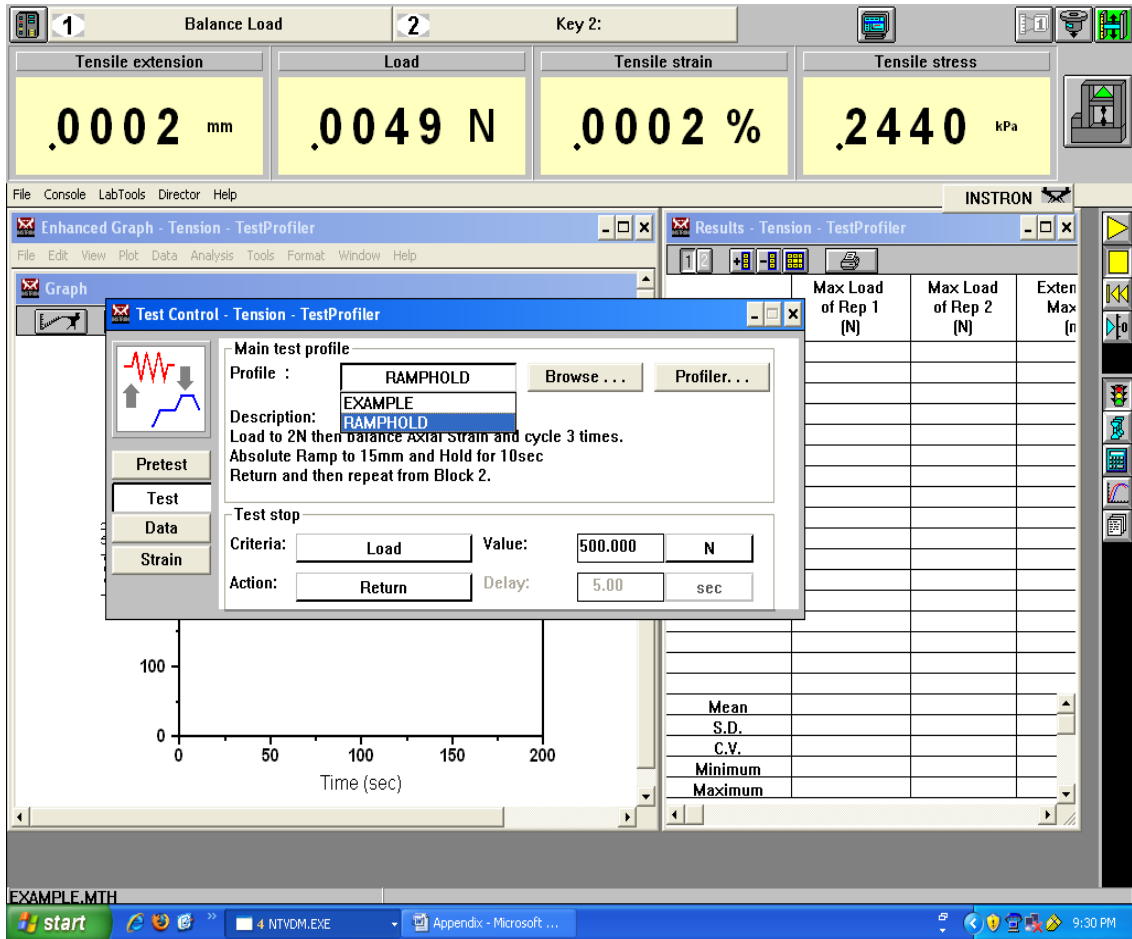
Repeat step 5 for all even numbered blocks with all the parameters constant for all.

Once the parameters have been set for all the blocks, we can save this method, so that we don't have to give the specifications every time we open this test. So save method by clicking on the file menu as shown below. And give it a name (RampHold)



So next time you open the Test control you can see this method in the drop down box as shown below.

You can select that method and proceed with the test directly.



In the test tab of test control make sure the criterion under test stop is set. Change the Criteria to time and give the value at which you want the test to stop. In this case the time was set to 300 seconds. The time depends on the duration you gave in the hold blocks. Put the value to be about 2 seconds higher than your test time.

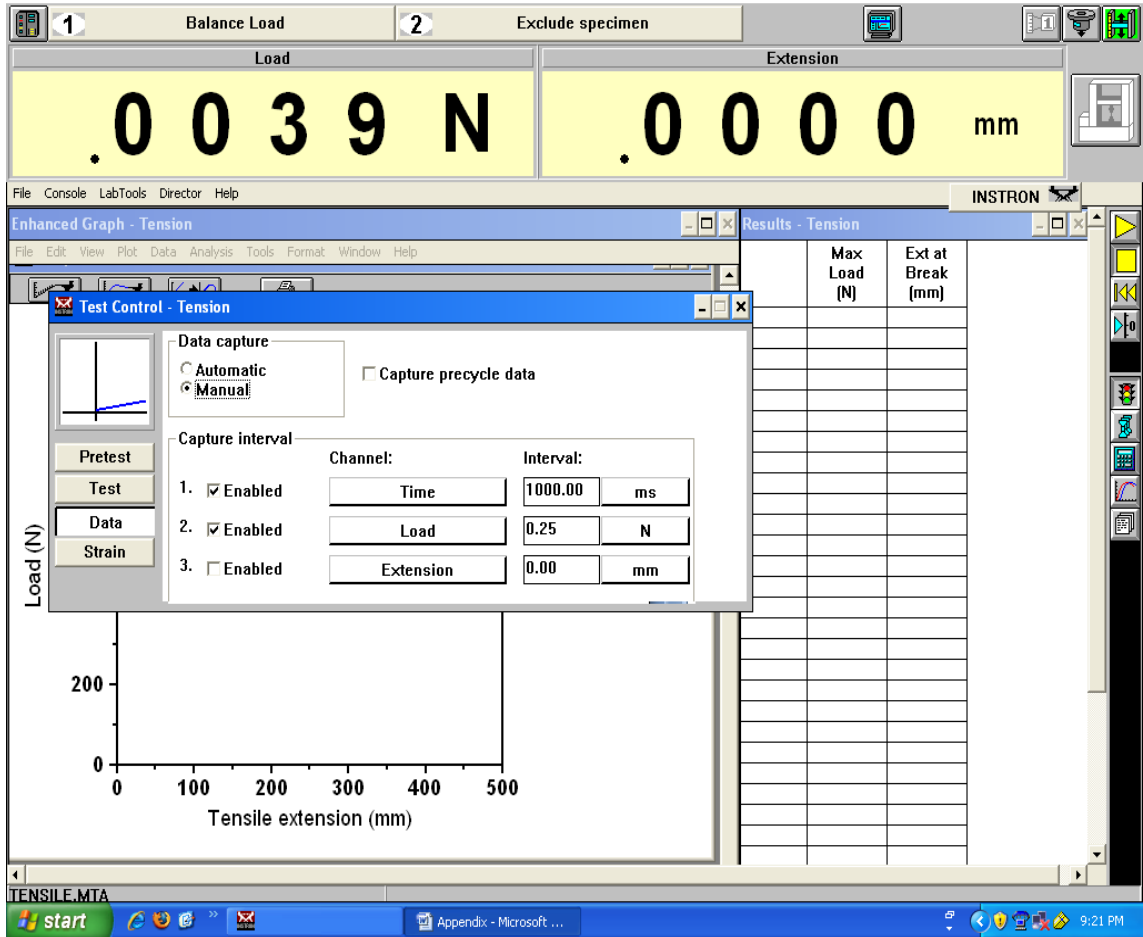
Once the specifications are given also give the specimen details by clicking on the Sample Lab tool as mention in Step 3 of the tensile test.

Step 6

You can also specify the number of data points you want to collect while the test is going on. The Data button is present in the Test control window of any test. For this test it is shown below. The data points is set to automatic usually as shown below.

The screenshot displays the INSTRON software interface for a tension test. At the top, two tabs are visible: '1 Balance Load' and '2 Exclude specimen'. Below these, two large digital displays show '0039 N' for Load and '0000 mm' for Extension. The main window contains several panels: 'Enhanced Graph - Tension' (top left), 'Results - Tension' (top right), and 'Test Control - Tension' (center). The 'Test Control' window is open, showing 'Data capture' set to 'Automatic' and 'Capture precycle data' unchecked. Under 'Capture interval', three channels are listed: 1. Time (1000.00 ms), 2. Load (0.25 N), and 3. Extension (0.00 mm). A graph at the bottom left plots 'Load (N)' on the y-axis (0 to 200) against 'Tensile extension (mm)' on the x-axis (0 to 500). The 'Results' table on the right has columns for 'Max Load (N)' and 'Ext at Break (mm)'. The Windows taskbar at the bottom shows the 'start' button, system tray icons, and the time '9:20 PM'.

You can select the manual option and give the time and/or load intervals at which you want data to be collected as shown below. Make sure you check the criteria that you want to be included. For example if you just want time interval then check that tab only or if you want both time and load intervals then check both of them as shown below.

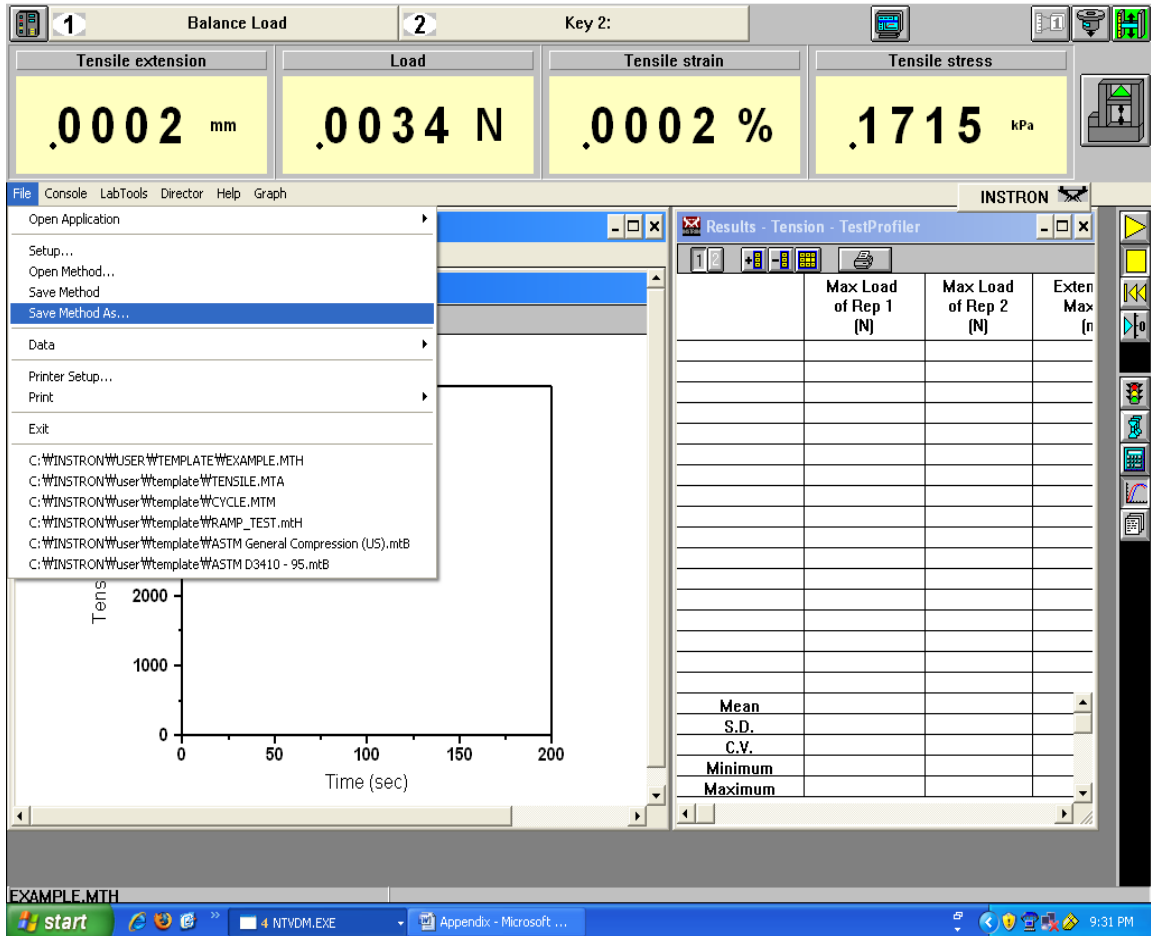


Setting up the number of data points you want is same for any test (tensile, cyclic, ramp-hold, etc.)

Step 8

After steps 1-5 you can save the method which saves the test control and sample specifications when you open the test again. This saves time so that you don't have to give all details every time you open the test. The methods can be saved for all types of tests (cyclic, ramp-hold and tensile) in the same manner as shown below. You save the method after you give all the test control and specimen specifications.

File menu → Save method As



Then give a new name to the test method, this appears on the main menu next time you open Merlin or give the old name, it just replaces the old specifications. In this case it is a ramp and hold method. Don't forget to keep the file extensions while giving them a name.

The screenshot displays the INSTRON TestProfiler software interface. At the top, four yellow boxes show test parameters: Tensile extension (.0002 mm), Load (.0058 N), Tensile strain (.0002 %), and Tensile stress (.2882 kPa). Below these is a menu bar with options: File, Console, LabTools, Director, Help, Graph. A toolbar contains various icons for file operations and test control.

A 'Save Method As' dialog box is open, showing the following fields:

- File Name: ramp and hold.mth
- Description: (empty)
- Directory: c:\instron\user\template
- Drive: c:

The dialog also shows a file tree with folders: c:\, INSTRON, user, and template. Below the dialog is a graph showing 'Time (sec)' on the x-axis (0 to 200) and a y-axis with a value of 0. The graph area is currently empty.

On the right side, a 'Results - Tension - TestProfiler' window is open, displaying a table with the following columns: Max Load of Rep 1 (N), Max Load of Rep 2 (N), and Exten Max (n). The table is currently empty, with summary rows for Mean, S.D., C.V., Minimum, and Maximum.

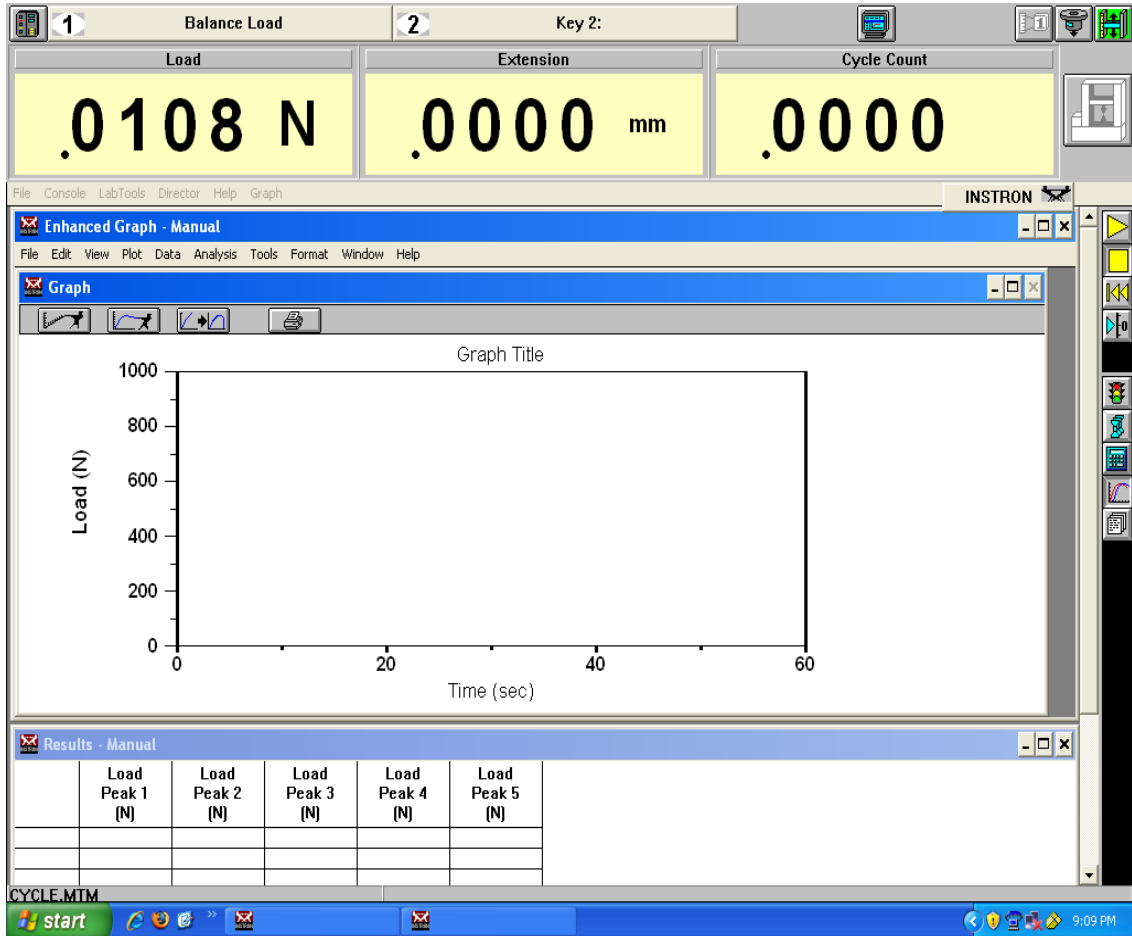
The Windows taskbar at the bottom shows the Start button, several open applications (5 NTVDM.EXE, Appendix - Microsoft ...), and the system clock (9:31 PM).

After saving the method, you can exit.

CYCLIC TEST

Step 1

Click on the cycle tab on the main menu. A window as shown below appears.



Define and enter the specifications of the specimen in the Sample lab tool as mentioned in other test methods.

Step 2

In the Test Control for cyclic test, we have to give limits between which the test has to be performed. Click on the Test profiler button and a window shown below appears.

The screenshot displays the INSTRON Test Control software interface. At the top, there are three main data fields: Load (-4.951 N), Extension (.0000 mm), and Cycle Count (.0000). Below these, a menu bar includes File, Console, LabTools, Director, and Help. The main window is titled "Test Control - Manual" and features a sidebar with buttons for Motion, Events, Cycling, and Data. A configuration window is open, showing settings for a cyclic test. It includes a "Channel" dropdown set to "Load", a "Value" field set to "56.00 mN", and a "Minimum" field set to "16.00 mN". The "End count" is set to "5" and is checked as "Enabled". The "Action" is set to "Stop". Below the configuration window is a graph showing Load (Y-axis, 0 to 400) versus Time (Sec) (X-axis, 0 to 60). The graph shows a single vertical line at 60 seconds. At the bottom, there is a "Results - Manual" window with a table for recording test results.

| Load Peak 1 (N) | Load Peak 2 (N) | Load Peak 3 (N) | Load Peak 4 (N) | Load Peak 5 (N) |
|-----------------|-----------------|-----------------|-----------------|-----------------|
| | | | | |

At the bottom of the screen, the Windows taskbar shows the "start" button, several application icons, and the system tray with the time 12:05 PM and the filename "Document1 - Microsof...".

You can give the limits and their units depending on your type of materials and the result you desire. In this case I have given load limits as shown below. And its respective units.

The screenshot displays the INSTRON Test Control software interface. At the top, there are three main data fields: **Load** showing **-4.951 N**, **Extension** showing **.0000 mm**, and **Cycle Count** showing **.0000**. Below these is a menu bar with options: File, Console, LabTools, Director, Help.

The main window is titled "Test Control - Manual" and contains a configuration panel for "Motion" and "Events". The "Motion" section has an "Enabled" checkbox. The "Events" section includes a table for setting limits:

| Channel: | Value: | Unit: |
|------------------------------------|--------|-------|
| Maximum: Load | 56.00 | mN |
| Minimum: Extension Strain [Exten.] | 16.00 | mN |

Below the table, a dropdown menu is open, listing "Load", "Stress", and "Strain 1". To the right of the table, there is an "End count" section with an "Enabled" checkbox and a value of "5", and an "Action:" dropdown set to "Stop".

A graph is visible below the configuration panel, with "Load" on the y-axis (ranging from 0 to 400) and "Time (Sec)" on the x-axis (ranging from 0 to 60). The graph shows a single vertical line at approximately 56.00 mN.

At the bottom of the window, there is a "Results - Manual" section with a table for recording peak values:

| Load Peak 1 | Load Peak 2 | Load Peak 3 | Load Peak 4 | Load Peak 5 |
|-------------|-------------|-------------|-------------|-------------|
| (N) | (N) | (N) | (N) | (N) |

The Windows taskbar at the bottom shows the "start" button, several application icons, and the system tray with the time "12:05 PM".

After you give the limits make sure you check the enabled field as shown below. If the enabled field is not checked then the program doesn't take those limits while running the test.

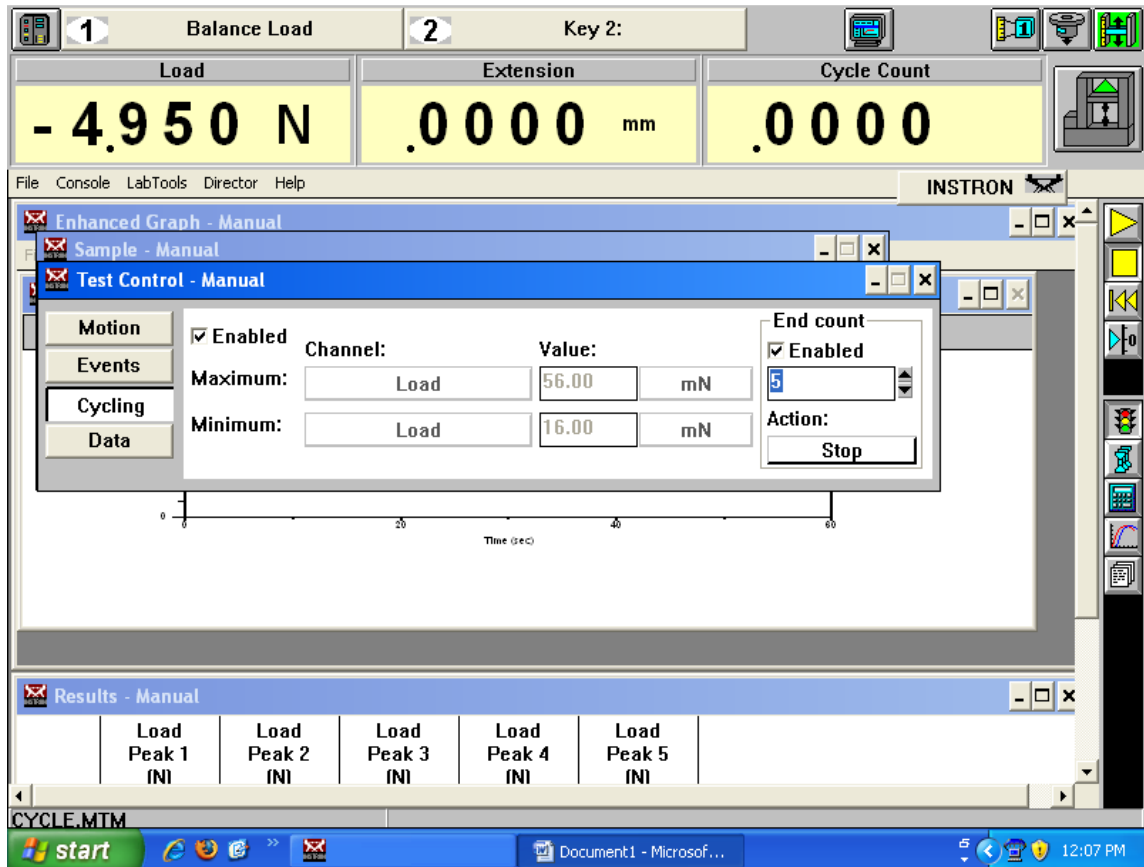
The screenshot displays the INSTRON Test Control software interface. At the top, there are three main data fields: Load (-4.950 N), Extension (.0000 mm), and Cycle Count (.0000). Below these is a menu bar with 'File', 'Console', 'LabTools', 'Director', and 'Help'. The main window is titled 'Test Control - Manual' and features a sidebar with 'Motion', 'Events', 'Cycling', and 'Data' options. A configuration window is open, showing 'Enabled' checked for both Maximum and Minimum load limits. The Maximum load is set to 56.00 mN and the Minimum load is set to 16.00 mN. The End count is set to 5 and the Action is Stop. Below the configuration window is a graph showing Load vs. Time (sec). At the bottom, there is a 'Results - Manual' window with a table for peak data.

| Load Peak 1 (N) | Load Peak 2 (N) | Load Peak 3 (N) | Load Peak 4 (N) | Load Peak 5 (N) |
|-----------------|-----------------|-----------------|-----------------|-----------------|
| | | | | |

CYCLE.MTM

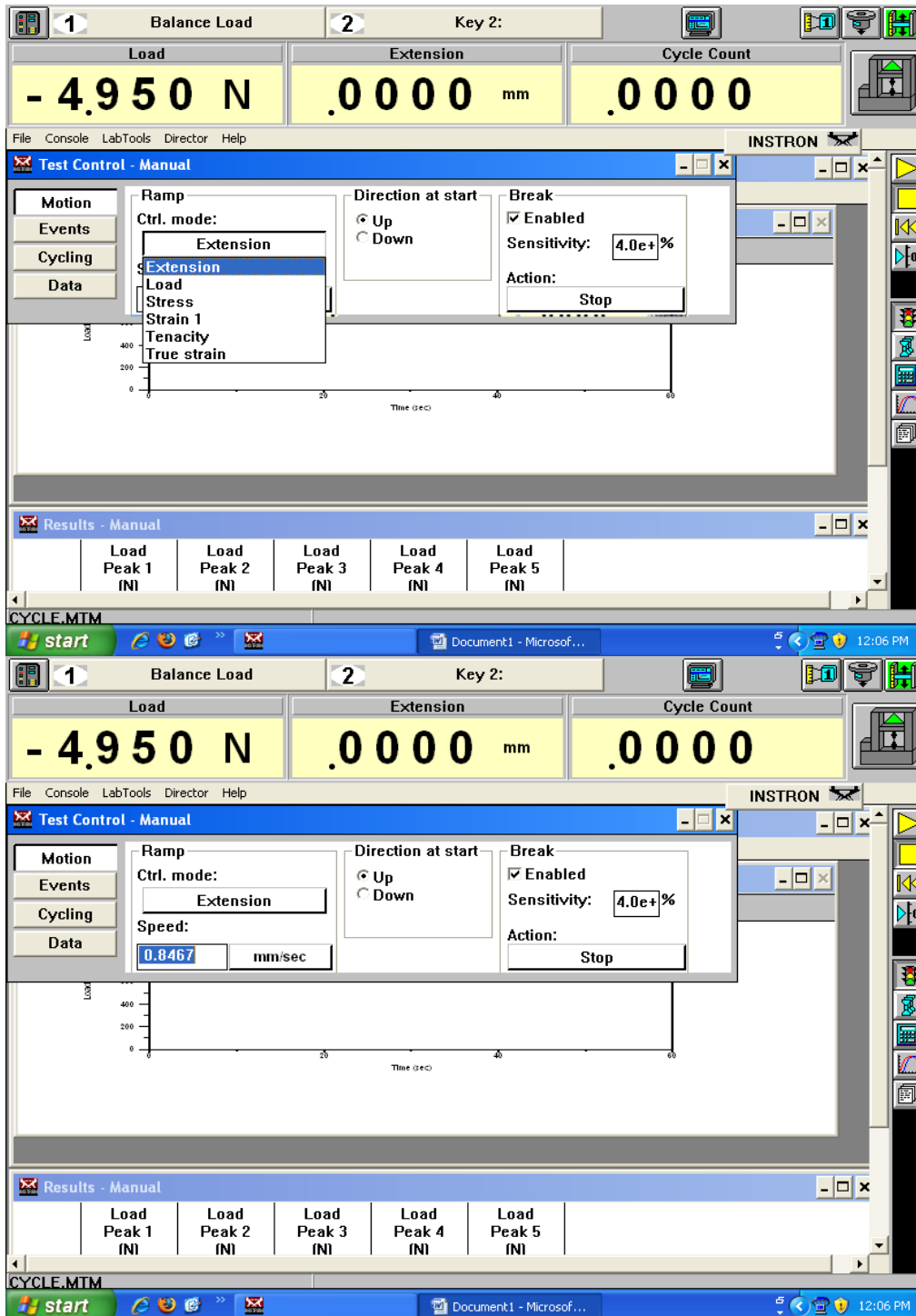
start | Document1 - Microsof... | 12:06 PM

In the same tab you can enter the number of cycles you want and check the enabled field as shown below.



Step 3

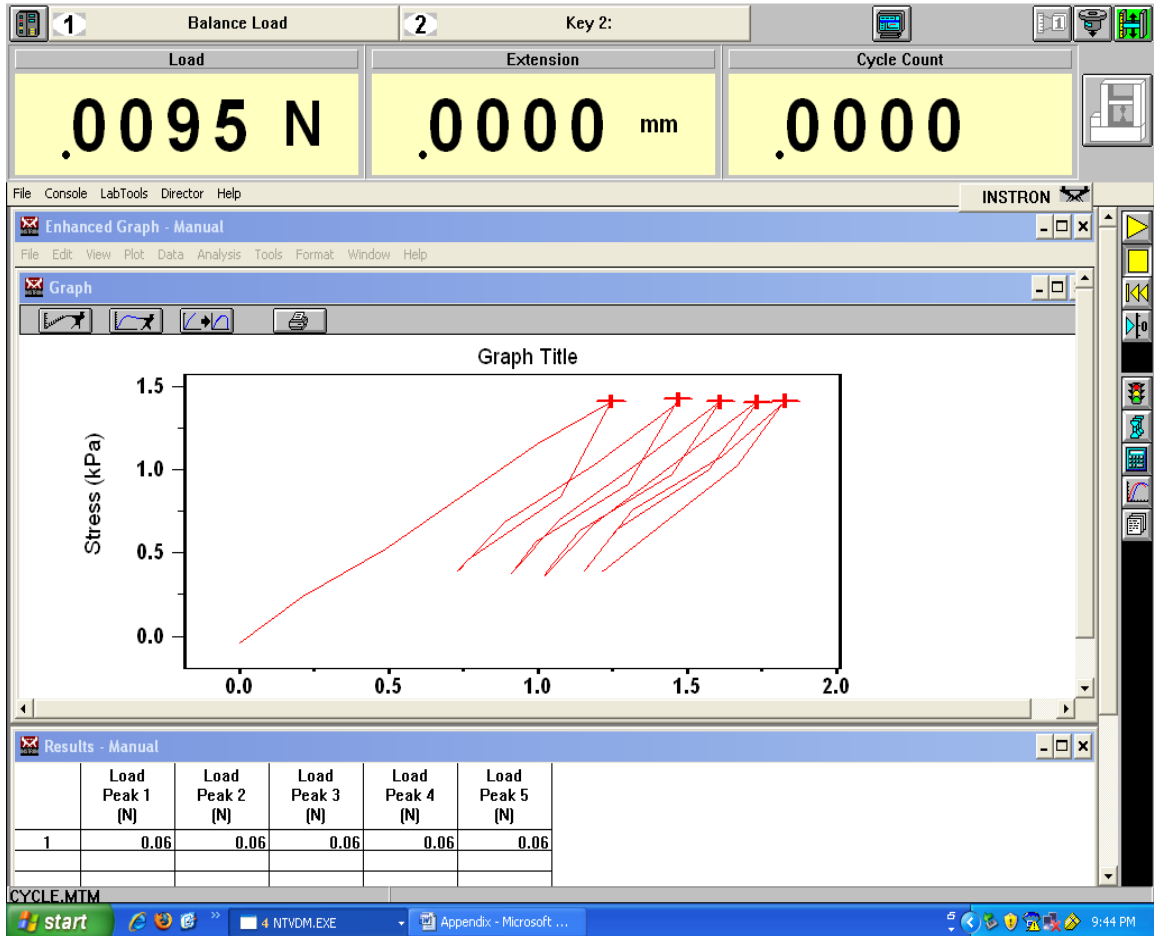
You can give the rate at which you want the sample to be pulled during cyclical testing by clicking on the Motion tab as shown below. And give the value of extension. Or you can also change the control mode.



You can also give the number of data points you want as mentioned previously in other test methods by clicking on the data button.

Step 4

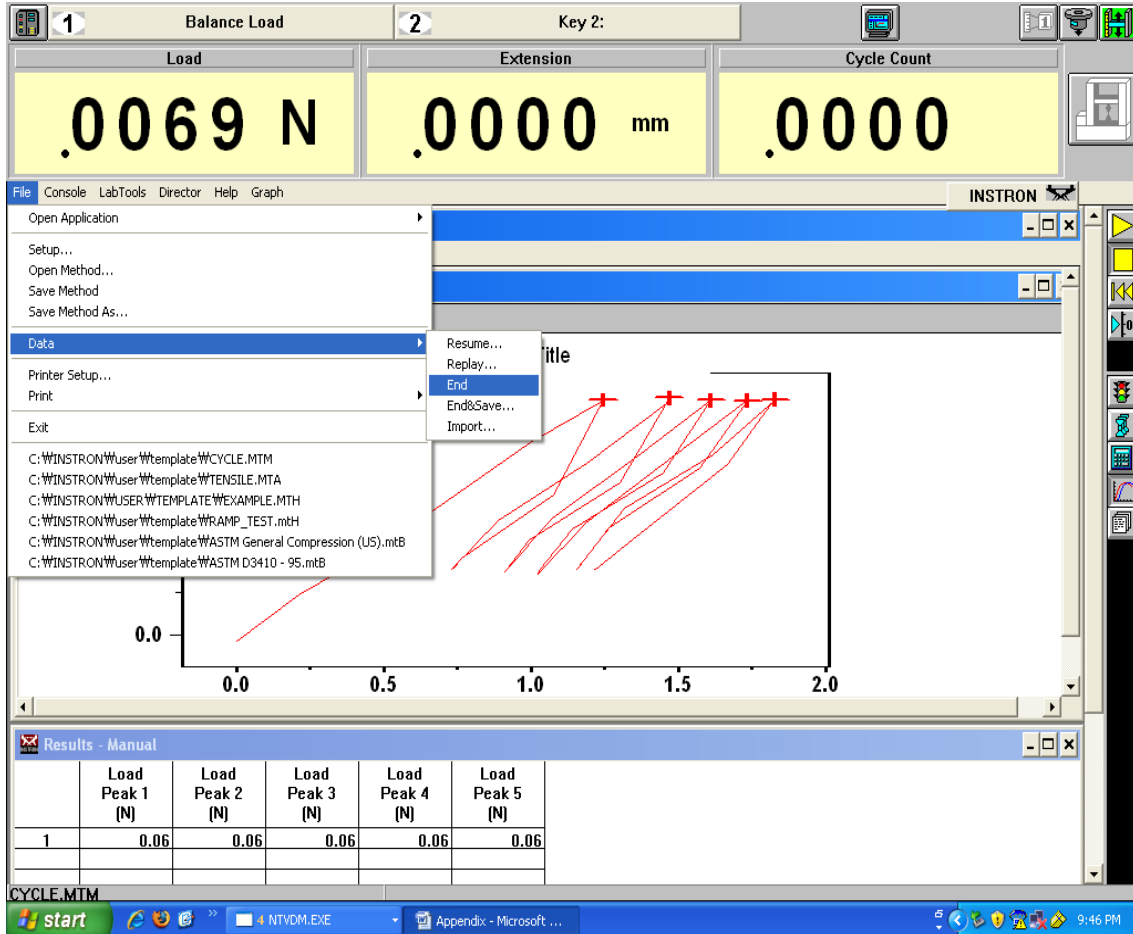
After all the specifications have been mentioned, reset the gauge length and click balance load and click play. The cyclic test gives a result as shown below.



You can save data as mentioned in Step 5 of tensile Test and/or save method as mentioned in step 6 of the stress-relaxation test.

Step 5

If you don't want to save data for any test or need a new page you can just go to File menu → Data → End, as shown below. This is common to any type of test. Remember this will not save any data.



After the test you can exit.

VITA

SWAPNIKA RATAKONDA

Candidate for the Degree of

Master of Science

Thesis: ASSESSING VISCOELASTIC PROPERTIES OF CHITOSAN SCAFFOLDS
AND VALIDATING SEQUENTIAL AND CYCLICAL TESTS

Major Field: Chemical Engineering

Biographical: Born on 6th of March, 1988 at Eluru, Andhra Pradesh, India.

Education: Graduated from Kendriya Vidhyalaya, Andhra Pradesh, India in May 2005; received a Bachelor of Technology degree in Chemical Engineering from B. V. Raju Institute of Technology (Affiliated to Jawaharlal Nehru Technological University), Andhra Pradesh, India in May 2009

Completed the requirements for the Master of Science in Chemical Engineering at Oklahoma State University, Stillwater, Oklahoma in December, 2011.

Experience: Worked as an Intern Researcher at Defense Metallurgical Laboratory, India from May-July 2008 and at Dr. Reddy's Laboratories, India from December 2008-April 2009.

Was employed as a Teaching Assistant from August 2009-May 2011 and as a Graduate Research Assistant from August 2009-December 2011 at Oklahoma State University.

Name: SWAPNIKA RATAKONDA

Date of Degree: December 2011

Institution: Oklahoma State University

Location: Stillwater, Oklahoma

Title of Study: ASSESSING VISCOELASTIC PROPERTIES OF CHITOSAN
SCAFFOLDS AND VALIDATING SEQUENTIAL AND CYCLICAL
TESTS

Pages in Study: 97

Candidate for the Degree of Master of Science

Major Field: Chemical Engineering

Scope and Method of Study:

We evaluated and modeled the viscoelastic characteristics of chitosan and chitosan gelatin scaffolds prepared using a freeze-drying technique. Chitosan and chitosan-gelatin solutions (0.5 wt% and 2 wt%) were frozen at -80°C and freeze dried. Using the scaffolds, uniaxial tensile properties were evaluated under physiological conditions (hydrated in Phosphate Buffered Saline at 37°C) at a crosshead speed of 0.17 mm/s. From the break strain, limit of strain per ramp was calculated to be 5% and the samples were stretched at a strain rate of 2.5 %/s. Ramp and hold type of stress relaxation tests were performed for five successive stages.

Findings and Conclusions:

Chitosan and chitosan-gelatin showed nearly 90% relaxation of stress after each stage. The relaxation behavior was independent of the concentration of chitosan and gelatin. Also, changes in the microstructure of the tested samples were evaluated using an inverted microscope. The micrographs acquired after relaxation experiments showed orientation of pores suggesting the retention of the stretched state even after many hours of relaxation. Based on these observations, a model containing i) a hyper-elastic spring (containing two parameters) and ii) retain pseudo components (containing three parameters) were developed in Visual Basic Applications accessed through MS Excel. The models were used to fit the experimental stress-relaxation data and the parameters obtained from modeling were used to predict their respective cyclic behaviors, which were compared with cyclical experimental results. These results showed the model could be used to predict the cyclical behavior under the tested strain rates. The model predictions were also tested using cyclic properties at a lower strain rate of 0.0867%/s (5%/min) for 0.5 wt% scaffolds but the model could not predict cyclical behavior at a very slow rate. In summary, this approach can be followed to select the best pseudo-component model that can be used to model sequential strain-and-hold stage and predict cyclical properties for the same strain rate of a particular scaffold.

ADVISER'S APPROVAL: Dr. Sundar Madihally
